

OPEN ACCESS

EDITED BY Sergio Maldonado, Tecnologico de Monterrey, Mexico

REVIEWED BY Janaka Bamunawala, Tohoku University, Japan Santosh G. Thampi, NIT Calicut, India

*CORRESPONDENCE
Manuel Cobos
mcobosb@ugr.es

RECEIVED 19 May 2025
ACCEPTED 05 August 2025
PUBLISHED 02 September 2025
CORRECTED 29 September 2025

CITATION

Otiñar P, Cobos M, Santana M, Millares A and Baquerizo A (2025) A probabilistic methodology for the projection of flooding and erosion processes in the coastal zones of Andalusia (Spain) throughout the 21st century. *Front. Mar. Sci.* 12:1631041.

COPYRIGHT

© 2025 Otiñar, Cobos, Santana, Millares and Baquerizo. This is an open-access article distributed under the terms of the Creative Commons Attribution License (CC BY). The use, distribution or reproduction in other forums is permitted, provided the original author(s) and the copyright owner(s) are credited and that the original publication in this journal is cited, in accordance with accepted academic practice. No use, distribution or reproduction is permitted which does not comply with these terms.

A probabilistic methodology for the projection of flooding and erosion processes in the coastal zones of Andalusia (Spain) throughout the 21st century

Pedro Otiñar, Manuel Cobos*, Marcus Santana, Agustín Millares and Asunción Baquerizo

Environmental Fluid Dynamics Group, Andalusian Institute for Earth System Research (IISTA), Granada. Spain

The increasing availability of climate projections has fostered the study of potential climate change impacts on coastal areas. In this context, we propose a general methodology to obtain joint probabilistic projections of coastal erosion and flooding in a climate change scenario, spanning decadal timescales and spatial extents of hundreds of kilometers. It has been implemented for the period of 2025-2100 along over 290 km of the Mediterranean Andalusian coast (Spain), characterized by a semiarid climate where there is a variety of coastal morphologies that include deltaic systems, natural pocket and headland bay beaches as well as other coastal landforms created in the shelter of marine structures. The methodology integrates: (1) the random character of climate and its intrinsic variability with a non-stationary multimodel ensemble approach; (2) the combined effect of maritime and hydrological events on the coast; (3) the availability of sediment and its 3D spatial layout, as well as its granulometry and degree of consolidation; (4) the sediment supply from rivers and ephemeral watercourses and (5) the presence of infrastructures that interfere with the hydrodynamic and sedimentary processes, such as dams in the river course, harbors, breakwaters, buildings and promenades. The methodology adequately emulates erosion and sedimentation patterns across various temporal scales, from individual events to long-term trends. Results for the high-emissions Representative Concentration Pathway scenario known as RCP 8.5 are illustrated at Guainos Beach, where it is found that the coastline adjusts to evolving wave climate conditions and sea level rise, exhibiting a decreasing trend in beach area primarily associated with sea level rise with intra-annual fluctuations superimposed during the early decades. Over time, the role of wave climate diminishes, and sea level rise becomes the dominant force, with a noticeable shift in the relative influence of forcings occurring around 2045 -2050. Compound flooding analysis reveals strong monthly variability in flood probability, especially at the river mouth and adjacent low-lying areas.

KEYWORDS

coastal erosion, coastal flooding, climate change impact, uncertainty assessment, hydro and morphodynamic processes

1 Introduction

The threat posed by climate change (CC) on the coast is taking on an increasingly significant role today and on the agenda of policy makers and coastal managers. Advanced models indicate that by the end of the century, significant changes in climate will occur. In addition to sea level rise (SLR), variations in maritime climate, precipitation patterns, and consequently, river flow and sediment supply, are expected (Fox-Kemper et al., 2021; Ranasinghe et al., 2021; Cooley et al., 2022). However, these changes in sediment dynamics are not solely driven by climate but are also strongly influenced by human activities. Interventions in river catchments such as dams, water abstraction, and land use changes - as well as coastal infrastructures like harbors, breakwaters, and promenades, can significantly alter sediment supply and disrupt natural coastal processes (Yang et al., 2020). Some impacts of human interventions on coastal morphology have not yet fully manifested. By 2100, these changes driven by human activity will be exacerbated by fluctuating sediment availability and climate variability across all global change scenarios (Caretta et al., 2022). In this context, coastal management decisions should be guided by well-informed coastal evolution plans that account for the scientific advancements made regarding future climate and the modelling of processes, as well as for the legal framework of each country. Despite the research advances and the raising concern of the administration, the transfer of knowledge between the academic and non-academic worlds is not as effective as desirable (Magaña et al., 2020). As a result, the implementation of local, urgent, and poorly informed decisions that disregard the complexity of coastal systems and the effects of changing global climate conditions is further hindered by legal and administrative frameworks that are misaligned with the insights of the scientific community.

In Andalusia (Spain), the service of the regional government's department responsible for authorizing the use and occupation of the coastal zone has promoted the development of a methodology to study the spatial and temporal variability of the coast in a CC scenario. The methodology has been implemented along the approximately 1,000 km of coast in the region. This initiative, which was launched in 2019, was carried out as part of two projects that were awarded to the University of Granada (UGR) and the Temporary Joint Venture (TJV) Estudio 7 – SandS. The UGR was responsible for developing the general methodology, coordinating the work, and implementing it in the provinces of Granada and Almería. Meanwhile, the TJV implemented it in the provinces of Huelva, Cádiz and Málaga.

This article presents the methodology developed within the framework of the so called ICCOAST project and its application in the coastal provinces of Granada and Almería.

Most of the research advances regarding the modelling of longterm coastal processes at study sites used reduced-complexity evolution models with simple geometries and stationary input conditions. Baquerizo and Losada (2008) highlighted that coastal morphology is the result of the random occurrence of storm and non-storm events and that those deterministic approaches cannot cope with the inherent randomness of the processes. Therefore, any predictive model for the evolution of the littoral zone over years or decades must be based upon statistical tools capable of dealing with the uncertainty of the prognosis. Some works have addressed this problem in the last decades. Vrijling and Meijer (1992) put the focus on this question and used Monte Carlo simulations to illustrate how to assess the probability distribution of the shoreline position for an idealized coast with assumed theoretical distributions of the forcing random variables. Reeve and Spivack (2004) introduced the use of statistical moments to forecast coastline evolution and its variability due to wave climate. In the direction of Vrijling and Meijer (1992); Payo et al. (2004) proposed a general methodology for the assessment of intrinsic uncertainty to be applied for the longterm prediction of the evolution of a certain morphological feature driven by climatologic agents, suitable to be applied, with forecasting purposes, to morphodynamic problems evolving in time and space. In their application to an ideal morphology, they used an analytical one-line solution obtained by Payo et al. (2003) forced with different equally likely wave climate time series realizations. Later approaches included the alongshore variability of sediment transport as well as the impact of a source of sediment due to river discharges (Losada et al., 2008). A probabilistic approach using a Monte Carlo wave climate simulation and a one-line model was performed by Wang and Reeve (2010) to assess long-term beach evolution in the vicinity of detached breakwaters. Ruggiero et al. (2007) also used a one-line model forced with several wave climate scenarios and different sediment supply boundary conditions to obtain probability density functions of shoreline position. Callaghan et al. (2008) analyzed extreme values of beach erosion with estimations made from simulated wave climate through a structural function based on an equilibrium profile concept. In the same line, Davidson et al. (2010) used synthetic times series to analyze the statistical behavior of the shoreline evolution with a beach profile model. Later, Ranasinghe et al. (2012) proposed a model to study long term coastal recession due to the combined action of storms and SLR in a beach profile. Stripling et al. (2017) used synthetic wave and river discharge scenarios, generated via Monte Carlo methods, to conduct a probabilistic analysis of shoreline evolution on a flat beach in the presence of a groyne or a sediment source. Meanwhile, Ding et al. (2018) developed a probabilistic framework based on Monte Carlo simulations that combines a stochastic wave climate generator with a shoreline evolution model to simulate the shoreline response along an idealized coast.

Most of the approaches address intrinsic uncertainty; however, model errors also introduce the so-called epistemic uncertainty (Vitousek et al., 2021). In relation with the later one, Vitousek et al. (2021) used an ensemble Kalman filter model to assess intrinsic uncertainty of coastal changes in a beach profile and to address epistemic uncertainty. Toimil et al. (2021) made long-term multiensemble coastal erosion projections emphasizing the visualization of the uncertainty cascade and the contribution of various uncertainty sources to the overall uncertainty. Thiéblemont et al. (2021) proposed an extra-probabilistic framework for obtaining shoreline projections that consider both intrinsic and epistemic uncertainties.

Some works faced the modelling of large-scale coastal stretches. Among them, the work by van Maanen et al. (2016) who used integrated models that gather different approaches to deal with a diverse coast of about 70 km at the east of England. Vitousek et al. (2017) presented CoSMoS-COAST model that includes longshore and cross-shore transport and studied with it the evolution of about 500 km of coast for a hindcast period. The model was fed with wave climate and SLR and uses historical shoreline information to improve estimates with a Kalman filter approach that parametrizes unresolved processes.

In the last years, efforts are focusing on making projections of CC induced impacts on the coast. One of the pioneering research projects is due to Zacharioudaki and Reeve (2011) who made a statistical analysis of shoreline variation of an ideal beach using a one-line model forced with different 30 years long wave climate projections. Their analysis focused on monthly and seasonal changes departing from a fixed position as the shoreline was set back to its initial shape after each single month or season. Panzeri et al. (2012) presented a GIS-based tool designed to simulate shoreline evolution and assess coastal vulnerability under changing wave climate and sea level rise scenarios. The tool enables probabilistic and scenario-based analyses through the integration of wave propagation models and shoreline response models, supporting comparative evaluations of long-term coastal impacts. Wainwright et al. (2015) analyzed long-term trends of coastline recession due to present day sediment budget and sea-level rise as well as the short-term with the method by Ranasinghe et al. (2012) and studied their combined effect in Narrabeen beach (Australia). More recently, Toimil et al. (2017) proposed a methodology to study recession due to waves, storm surge and SLR with a cross-section-based equilibrium model and applied it to several beaches along the Spanish north coast. Alvarez-Cuesta et al. (2021a) proposed a methodology that uses multimodel projections of climate to calculate ensemble shoreline changes over a 40 km of a coastal stretch using the shoreline evolution model presented in Álvarez-Cuesta et al. (2021b) that accounts for long-shore and cross-shore processes as well as for SLR and unresolved processes with a data assimilation technique as in Vitousek et al. (2017). Vitousek et al. (2021) obtained shoreline projections in Tairua beach (New Zealand) and reduced model and intrinsic uncertainties using an ensemble Kalman filter cross-shore model. d'Anna (2022) followed a similar approach for Truc Vert beach (France) and analyzed the relative impacts of uncertain input variables on shoreline changes. Toimil et al. (2023) focused on the estimation of projections of coastal flooding coupled with coastal erosion along a coastal Mediterranean stretch.

In addition to those studies, there are conceptual works that have highlighted the main challenges to be faced in this line of research and inspired some of the mentioned works. Among them, it is remarkable the work by Ranasinghe (2016) who made a review aimed at facilitating best practice to quantify physical impacts of CC on coasts at local scales (<10 km). In that work, he pointed out that, on sandy beaches, those impacts are driven by SLR as well as wave conditions and river flow and proposed a methodological framework to assess local scale impacts. More recently, Toimil

et al. (2020) reviewed the challenges of studying the risks of global changes in coastal zones, highlighting, among others, the multi-impact assessment considering climate change as well as other socio-economic pathways. Splinter and Coco (2021) outlined the present condition of shoreline modelling for periods less than a century and offered insights into future challenges and opportunities. Among other, they highlighted the importance of dealing with non-stationarity and the limitation of the assumption of unlimited sediment supply.

The present work is part of the ICCOAST project which objective was the development of a methodology to make joint projections of erosion and flooding coastal impacts due to CC along the Andalusian coast. In this article and in a companion paper by Otiñar et al. (2025), we present its implementation to the Andalusian coastal provinces of Granada and Almería, located along the Mediterranean coast for the 21st century (2025 - 2100), under the RCP 8.5 climate scenario. To the authors knowledge, the methodology addresses for the first time some of the challenges highlighted in theoretical works such as, the sediment supply by watercourses, the geological setting, and the non-stationarity of climate. The differences with previous works can be assessed in Supplementary Table S1 of the Supplementary Material (SM) that summarizes the main characteristics of this research and the abovementioned methodologies. Among them, it is remarkable the way of dealing with the multimodel approach, in which future climate is dealt with a multivariate non-stationary multimodel ensemble characterization (Lira-Loarca et al., 2021) that differs from the approach by Toimil et al. (2021, 2023), Álvarez-Cuesta et al. (2021b) and Vitousek et al. (2021) who follow the methodological approach suggested by Ranasinghe (2016). We jointly consider maritime and hydrological agents for rivers and ephemeral river courses and their sediment supply as well as their effect on sea-levels and, therefore, the extension of flooding. They are treated with Guadalfortran model (Ávila, 2007; Losada et al., 2011) that solves Saint-Venant equations for non-stationary-1D flux. For ephemeral river courses, the catchments' contribution is estimated with a model that uses the Soil Conservation Service curve number method (SCS, 1956; Kumar and Vijay, 2003) fed with precipitation projections. Regarding the morphodynamic processes, we use a version of CoastalME (Payo et al., 2017), a shoreline reduced complexity evolution model that has been improved in collaboration with the British Geological Survey development team. The implementation of the methodology is illustrated with results from Guainos Beach. In a companion paper by Otiñar et al. (2025), we present the procedure for the statistical analysis of the results, aimed at facilitating informed decision making, and also present the overall results obtained along the analyzed coast.

The paper is organized as follows. Data and materials section include the description of the study site (Section 2.1), the models employed for reproducing the physical processes (Section 2.2) and the data used for the analysis (Section 2.3). The methodology is shown in Section 3, and the results of its application are gathered in Section 4. The Section 5 closes the paper with the discussion and conclusions.

2 Data and materials

2.1 Description of the study site

The Andalusian Mediterranean coast in the provinces of Granada and Almería lies at the foothills of coastal mountain ranges (Figure 1). This region features rivers and seasonal streams that flow over steep terrain, forming deltaic zones or small coves at their mouths, which alternate with cliffs. It is characterized by a semiarid climate with marked interannual variability. The area includes natural regions that remain unaltered and legally protected, as well as others that have been heavily developed with urban settlements and the necessary infrastructures for the population. The coastal morphological types of that region include deltaic systems, natural pocket, and headland bay beaches as well as other coastal landforms created in the shelter of marine structures.

In terms of maritime forcing, the study area is microtidal, with tidal ranges typically less than 0.5 m, making the coastal dynamics primarily wave-dominated. The wave climate is characterized by moderate energy, with significant wave heights generally ranging between 0.5 m and 1.5 m, and maximum values exceeding 3 m during storm events. It is characterized by a bimodal directional pattern, with two dominant wave directions. Along the southern part of the Alborán Sea coast, the dominant wave directions are W–SW and E–SE, while along the more eastern sectors, dominant wave directions shift to E and S-SW. These wave conditions drive a bidirectional longshore sediment transport system, with alternating transport directions depending on seasonal storm patterns and wind regimes (Losada et al., 2011).

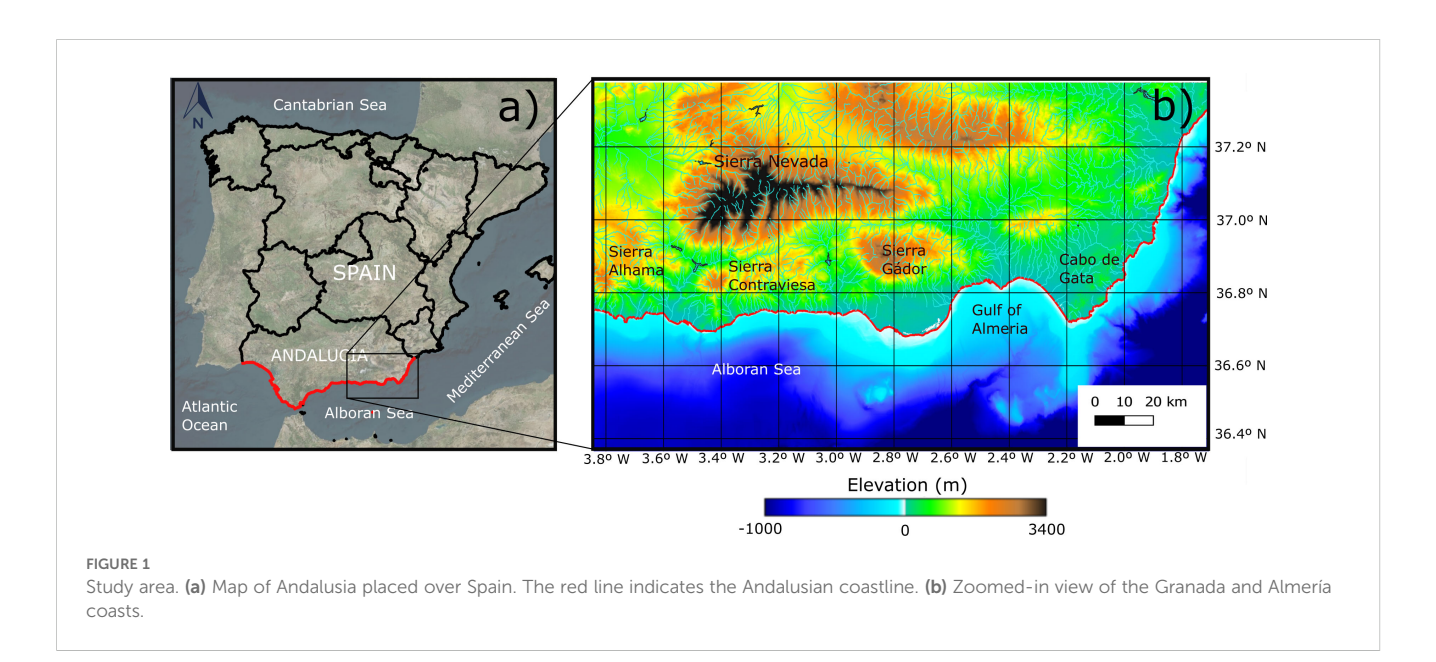
In terms of the landscape, the region is intersected by several small rivers and a few ephemeral watercourses. The main rivers are the Guadalfeo, Adra, Andárax, Carboneras, Aguas, Antas and Almanzora. Due to the semiarid climate, these streams typically have low annual discharges, but can experience flash floods during intense rainfall events, delivering pulses of sediment to the coastline (Millares et al., 2014). The Aguas River, the least significant in terms of flow, has typical annual discharges ranging from 2–10 MCM/year, while the Guadalfeo

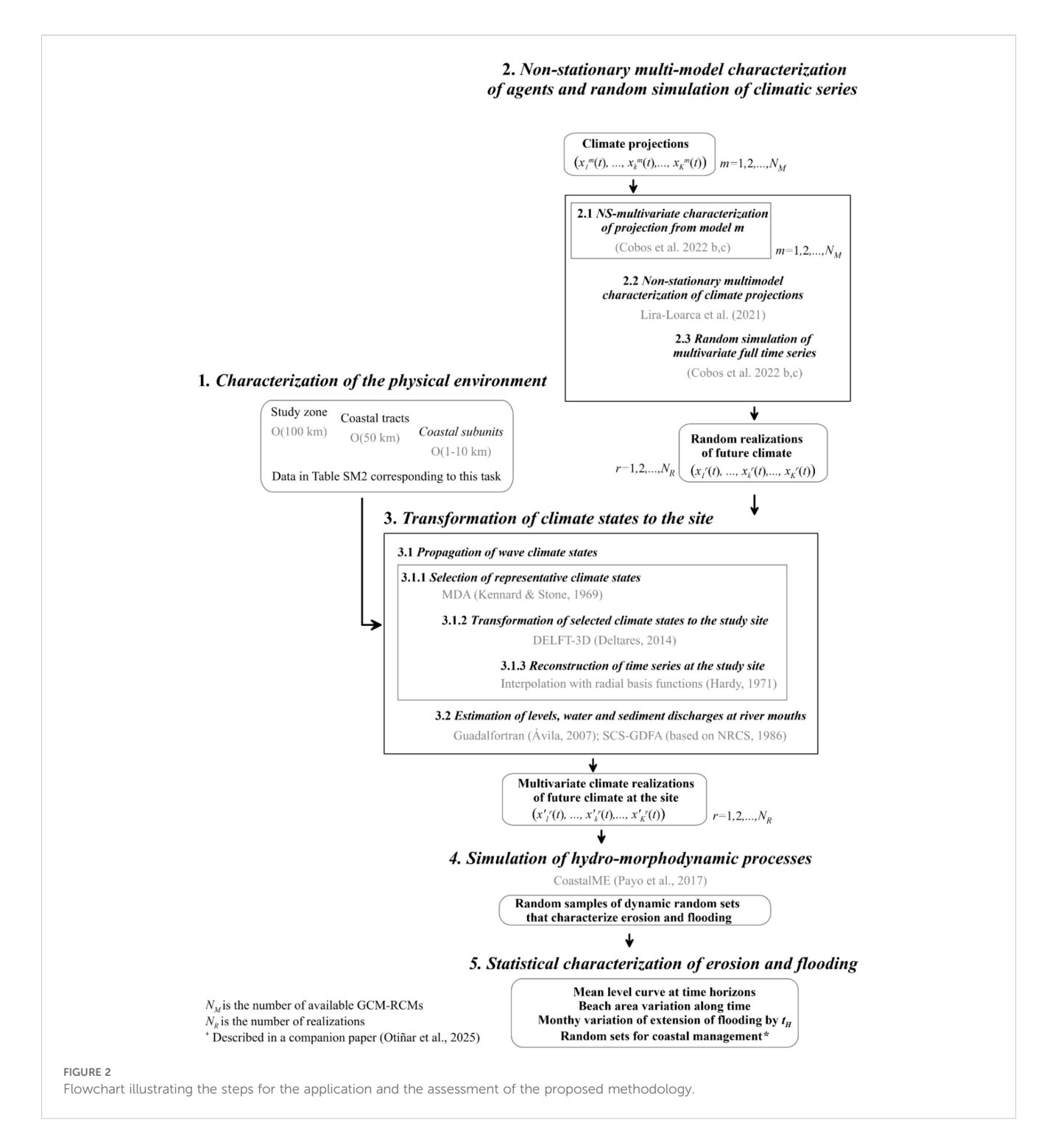
River, the most water-rich in the study area, has discharges ranging from around 100–150 MCM/year. Similar behavior is observed in the ephemeral watercourses, which are numerous and constitute a defining feature of the coastline in the provinces of Granada and Almería. Despite remaining dry for most of the year, they can supply substantial sediment loads during episodic events. The present analysis considers a total of 30 creeks due to their potential contribution to coastal sediment budgets. Although irregular, these sediment pulses play a crucial role in the sediment budget of coastal systems in semi-arid environments, where fluvial contributions are limited but highly episodic and intense.

The survival of beaches, particularly those affected by human interventions such as the construction of dams, promenades, and coastal infrastructures, strongly depends on the availability of seabed sediment and the presence of outcrops, which vary spatially (Cobos et al., 2022a). Their long-term behavior also depends on the temporal variability of atmospheric and wave climate. Precipitation events are scarce but intense (Cantalejo et al., 2024) and can supply significant amounts of sediment to the coast at the mouths of watercourses (Millares et al., 2014), which are then redistributed by sea storms, usually alternating in opposite directions (Losada et al., 2011). Sea climate severity also shows strong interannual variation.

2.2 Models to reproduce the physical processes and statistical techniques employed

We employed a range of numerical models to reproduce the physical processes, the main characteristics of which are summarized in Table 1. The Delft3D suite (Deltares, 2014) was used for wave propagation from deep water to depths of 20–25 meters. River and sediment discharges at watercourses were obtained using Guadalfortran (Ávila, 2007; Losada et al., 2011) and the SCS-GDFA model (Section 3 of SM), which was specifically coded and implemented to determine catchment contributions at





creeks and ephemeral rivers. The evolution of the shoreline was simulated using a version of CoastalME (Payo et al., 2017), a software package that allows for the simulation of morphological changes at decadal and longer time scales.

CoastalME model was updated for the ICCOAST project in collaboration with the British Geological Survey (UK) to account for: (1) the temporal variability of wave climate and sediment discharges from rivers and creeks; (2) the presence of rigid, non-erodible elements derived from geospatial cadastral information and the BTN25 database

(rows 12 and 14 of Supplementary Table S2), (3) seabed sediment availability, by incorporating six sediment layers whose thickness varies spatially and temporally depending on effective transport (row 9 of Supplementary Table S2); and (4) the extraction of intersection curves between sea level and terrain. The model was calibrated using satellite-derived shorelines extracted from LandSat 7 imagery during 2008-2015. For that purpose, a fully automated procedure was implemented using Google Earth Engine, following the methodology developed by Magaña et al. (2022). This approach applies an adaptive thresholding algorithm

TABLE 1 Description of models employed, and I/O data required in the methodology.

Model Description/Implementation	Input data	Output data
DELFT3D suite (Deltares, 2014) for wave propagation from deep waters to coastal subunits.		
It is a wave propagation model that accounts for non-linear wave components as well as non-stationary processes associated with tide and wind forcing, and their interaction with waves. It was implemented for each coastal tract over a curvilinear grid, which included higher-resolution grids for the regions closer to the shore within each considered subunit. It was used with the WAVE (Booij et al., 1999) and FLOW (Lesser et al., 2004) modules for the higher-resolution grids. The parameters employed were those obtained from the calibration carried out on the coast of Granada (Bergillos et al., 2017).	 ■ Topobathymetry ■ Wind waves (H_S, T_P, θ_m) ■ Wind (V_w, θ_w) ■ Mean sea level Information provided at deep water, with a 3h resolution. 	■ Wind waves (H_S, T_P, θ_m) At control points of coastal subunits at approximately 20–25 m depth with a 3h timestep.
SCS-GDFA model that uses the SCS-CN method to obtain surface flow and sediment supply at creeks and ephemeral rivers		
It estimates runoff with the SCS-CN method (SCS, 1956; Kumar and Vijay, 2003) and simulates the response of small basins with a discrete convolution integral that employs the unitary hydrograph of the SCS to obtain the surface flow (see Section 4 of SM). It was implemented in 30 ephemeral watercourses.	 Precipitation Soil features (converted to curve number) Catchment area Length of the mainstream to farthest divide Watercourse mean slope 	■ River discharge
Guadalfortran (Ávila, 2007, 2008; Losada et al., 2011) to obtain river and sediment discharges and sea level at relevant river mouths.		
It solves the Saint-Venant equations for non-stationary 1D flow and includes a water balance module to account for regulatory activities at dams. It uses the traditional sediment transport formulas [Bagnold (1966); Brownlie and Keck (1981), Meyer-Peter and Müller (1948) and Wilcock and Crowe (2003)]. It was implemented for the most relevant rivers (Guadalfeo in Granada, and Adra, Andarax, Carboneras, Aguas, Antas, and Almanzora in Almería). The parameters employed were those obtained from the calibration carried out for the Guadalfeo River (Ávila, 2007).	■ Topography ■ Freshwater river discharges (<i>Q</i>) along the main tributaries and dams. For creeks, input discharges come from SCS-GDFA outputs.	■ Water level along the main channel ■ Mean water current along the main channel and associated solid sediment discharge at the river mouth
Coastal Modelling Environment (Payo et al., 2017) to simulate hydrodynamic and sedimentary processes at the coast.		
It is a one-line model that estimates the sediment dynamics of a coastal stretch while conserving the total volume of sediment. It was used alongside CSHORE (Kobayashi, 2016) to model coastal hydrodynamic processes, including wave propagation, energy dissipation due to bottom friction and wave breaking, and sea-level variation. It was implemented for each coastal stretch.	 ■ Wind waves (H_S, T_P, θ_m) ■ Sea level (η) At control points of coastal subunits at approximately 20–25 m depth at 3h resolution ■ 3D spatial layout of rigid, non-erodible elements ■ Stratigraphy of seabed along the Andalusian coast (Torrecillas et al., 2024) 	■ Time variation of shoreline position ■ Time variation of topobathymetry

 H_{S} , significant wave height; T_{P} , peak period; θ_{m} , mean wave direction; V_{w} , wind intensity; θ_{w} , wind direction; η_{SLR} , mean sea level (due to SLR); η_{SS} , storm surge; η_{AST} , astronomical tide; η , sea level, including mean level, astronomical and meteorological tide due to wind and set-up.

based on the Normalized Difference Water Index (NDWI) and includes post-processing steps for spatial connectivity and noise filtering. Calibration involved minimizing the root mean square error between the shorelines extracted from satellite imagery and the shorelines simulated by the model at the same time points and aimed to adjust key parameters to accurately reproduce the hydrodynamics and morphodynamics of the study area, particularly with regard to the erosion resistance of platforms, cliffs and shallow zones.

MarineTools.temporal software (Cobos et al., 2022b) was used to perform a multi-model non-stationary characterization of climate time series and to generate multivariate realizations with simulation techniques (Cobos et al., 2022c).

2.3 Data

A variety of data sources were employed for the analysis of the physical environment and climate, as well as to provide input for the hydro-morphodynamical models. These included: (1) geographical data (e.g., topobathymetric data, land use distribution, hydrography); (2) geological data (spatial distribution of sediment thickness); (3) spatial distribution of structural elements (e.g., infrastructures, buildings, installations); (4) climate data—comprising historical observations, hindcasts, and climate change projections—related to wind waves, wind, precipitation, and river discharges; and (5) satellite imagery.

Key features such as data sources, variables used, and their spatial and temporal coverage and resolution are summarized in Supplementary Table S2 of the Supplementary Material. Further details on climate projections, the sediment thickness model, and satellite imagery are provided below.

2.3.1 Climate projections

Climate projection data consisted of realizations from multiple climate models, i.e., multivariate time series simulating potential future climate conditions under the Representative Concentration Pathway (RCP) associated with a total radiative forcing of 8.5 W/m² by the year 2100. Maritime projections (row 8 of Supplementary Table S2) were obtained from the PIMA Adapta project (Ramírez et al., 2019), available at a spatial resolution of less than 10 km along the Spanish coast. These time series were bias-adjusted and derived from eight combinations of global and regional climate models (GCM-RCM) for wave climate. For the same model combinations, wind and meteorological tide data were sourced from COPERNICUS (row 9 of Supplementary Table S2). Wind time series were bias-corrected using the Empirical Quantile Mapping method (Déqué et al., 2007; Michelangeli et al., 2009), the same approach applied to wave data in Ramírez et al. (2019), based on hindcast data and observations. Precipitation projections from EURO-CORDEX were obtained using five GCM-RCM combinations. Bias-adjusted River discharge projections (row 10 of Supplementary Table S2) were sourced from the E-HYPEcatch project (Donnelly et al., 2016) via COPERNICUS, based on four model combinations (REMO2009-MPI-ESM-LR, RCA4-HadGEM2-ES, RCA4-EC-EARTH, RACMO22E-EC-EARTH). Mean sea level projections were also obtained from the PIMA Adapta project (Ramírez et al., 2019).

2.3.2 Thickness model

The thickness model developed by Torrecillas et al. (2024) (row 5 of Supplementary Table S2) was specifically designed for this project to be integrated with CoastalME. It combines geological, geomorphological, bathymetric, and sedimentological data to map different sediment fractions along the Andalusian coast. The geological and geomorphological inputs include a geology layer, schematic boreholes, stratigraphic sequences, and cross-sections, all provided in raster format. Bathymetric data consist of elevation information, while sedimentological data describe seabed sediment layers. A total of eighteen physiographic zones were defined based on a generalized coastal characterization vector layer—seventeen overlapping and one additional unique zone. These zones were used to clip the mosaics, resulting in the generation of over 830 profiles representing approximately 7,225 km of interpreted shallow subsurface sections. For each zone, six sediment layers were created to distinguish between consolidated and unconsolidated materials, classified into fines (clays and silts), sands (0.063 mm < D_{50} < 2.0 mm), and gravels (D_{50} > 2.0 mm). Consolidated sediments refer to solid rock formed through metamorphism or cementation, including sedimentary rocks such as conglomerate, sandstone, siltstone, shale, and limestone. Unconsolidated sediments consist of loose material ranging from clay to gravel. Grain size distributions and the degree of consolidation were determined based on lithological descriptions from the source maps. The vertical arrangement of these materials follows a granulometric gradient: coarser consolidated sediments tend to be in deeper layers, farther from the water-soil interface, while finer, unconsolidated materials are found closer to the surface. Each layer is assumed to contain a well-mixed composition of the respective sediment types.

2.3.3 Satellite images

Satellite imagery from Landsat 7 (row 13 of Supplementary Table S2) was used to calibrate the CoastalME model. Images were selected following a rigorous quality assessment, excluding those with cloud cover exceeding 5% as well as most images containing data gaps (strips with no information) affecting more than 10% of the area. Shorelines were automatically extracted from the selected images using the methodology described in Magaña et al. (2022).

3 Methodology

The methodology assumes that, for a given realization of wave climate over a specific time interval, morphological changes can be analyzed as the cumulative effect of a sequence of climate states during which conditions remain approximately stationary (Baquerizo and Losada, 2008; Payo et al., 2008). This assumption enables the decoupling of hydrodynamic and morphodynamic processes, thereby reducing the complexity of the modelling approach (De Vriend et al., 1993). By repeating this procedure multiple times, it is possible to generate different, equally probable realizations and to analyze dynamic random sets related to coastal evolution and flooding occurrence.

For each realization, the methodology begins with an initial configuration of a specific coastal area, defined by bathymetry, terrain characteristics—such as sediment properties and land use—and the presence of infrastructures. Future climate projections derived from multiple combinations of GCM–RCM models are also known. The methodological steps are detailed below and illustrated in Figure 2.

3.1 Characterization of the physical environment

The analysis of the physical environment enabled the identification of distinct coastal tracts at a regional scale [O(50 km)], defined as sediment-sharing cells in accordance with Cowell et al. (2003). Within each cell, sediment availability, as well as sediment sources and sinks, were determined. These tracts were further subdivided into subunits at a local scale [O(1–10 km)], characterized by similar morphological features and exhibiting a comparable range of climatic variability, following the concept of "subsets" of maritime works defined in the Spanish Recommendations for Maritime Works (Losada, 2001, 2009). Within each tract, rivers and creeks that could potentially

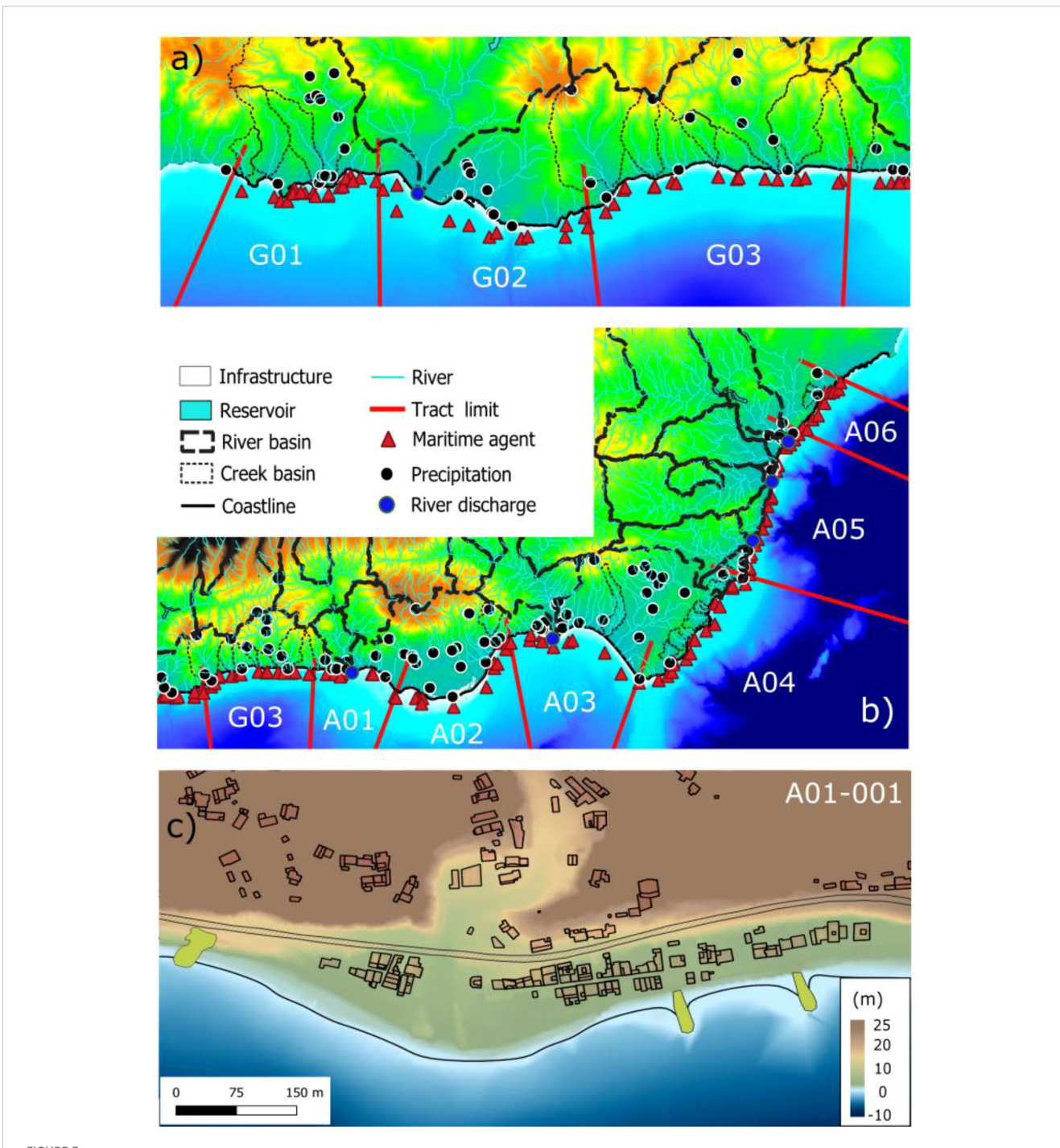


FIGURE 3
Characterization of the physical environment. Identification of coastal tracts and key physical features (including coastline, watercourses, basins, and reservoirs) in the Granada coast (a) and the Almería coast (b), along with the spatial distribution of climate data sources. (c) Detailed view of subunit A01-001, highlighting the infrastructure present at Guainos Beach (e.g., buildings, promenades, and breakwaters). The initial mean sea level is represented by a continuous thick black line, serving as a reference.

influence flooding and sediment supply were identified using data from Andalusia's Areas with Significant Potential Flood Risk (APSFR). These areas were defined through Preliminary Flood Risk Assessments (known as PFRA), conducted in alignment with EU Directive 2000/60/EC. Additional information was obtained from the coastal flood-prone area inventory developed as part of the Riskcoast project (Mateos et al., 2020a, b).

3.2 Multi-model characterization of agents and random simulation of climatic series

Time series with projections of wave climate, storm surge, wind characteristics, precipitation, and river water discharges were considered. A multi-model stochastic non-stationary characterization of future climate was performed (Lira-Loarca et al.,

2021). This methodology first involves a non-stationary characterization of univariate and multivariate climate for each individual GCM-RCM timeseries, consisting of: (i) the fitting of non-stationary marginal distributions to each random variable (Solari and Losada, 2012; Cobos et al., 2022c), and (ii) the assessment of short-term temporal dependence between wave climate variables using a stationary vector autoregressive (VAR) model. A Bayesian approach is then applied to the marginal distributions, where each random component is treated as a compound variable, with its distribution obtained as the weighted summation of the nonstationary distributions fitted to each GCM-RCM timeseries. This approach accounts for uncertainty regarding the true state of nature by considering that the time-varying parameters of the marginal probability models are themselves random variables. The temporal dependence of the compound variable at a given time, with respect to its previous values and, in the multivariate case, also the other variables, is obtained as the ensemble mean of the matrices that describe the parameters of the VAR model for the GCM-RCM timeseries. The random variables representing river discharge and precipitation were considered independent from the remaining variables $(H_S, T_p, \theta_m, V_w, \theta_w, \eta_{met})$ due to the unavailability of consistent climate projections from the same GCM-RCM model combinations. This assumption is nonetheless justified by the semiarid to arid nature of the river and creek basins in the study area, where fluvial discharges are infrequent events typically uncorrelated with wind wave storms (Losada et al., 2011).

Due to the lack of wave climate data for the period 2046–2080, an analysis using the aforementioned methodology of Lira-Loarca et al. (2021) was previously conducted for the periods 2026–2045 and 2081–2100. The comparison of their non-stationary empirical percentiles for the relevant variables revealed no statistically significant differences between these periods (<10 cm for wave height and <10° for mean wind direction). Data from the nearer period, 2026–2045, was therefore considered representative for the entire century and used throughout the analysis. This assumption aligns with the conclusion of Álvarez-Cuesta et al. (2021b), who assessed the same dataset for the Castellón coast and concluded that significant changes in wave climate are not expected.

The results of the statistical characterization were used to generate twenty new random multivariate time series that preserve the statistical properties of the original data (Cobos et al., 2022b). These series represent equally probable realizations of future climate conditions for each coastal subunit, spanning the analysis period from 2025 to 2100.

3.3 Transformation of climate states to the site

As part of this task, the climate conditions from the realizations were downscaled to the vicinity of the coastal subunits using models that simulate the physical processes. The characteristics and input/output data of these models are summarized in Table 1, along with additional numerical tools described in the following sections.

3.3.1 Propagation of wave climate states

Due to the computational cost of propagating wave climate states over the entire time series, a combination of physically based models and mathematical tools was employed. Specifically, 500 representative sea states-characterized by waves, wind, and sea level in deep water-were selected using the Maximum Dissimilarity Algorithm (MDA) (Kennard and Stone, 1969), which identifies, among all possible combinations of climatedefining variables, those that best represent the event space. The algorithm was applied to rescaled variables, with their variability range normalized to the [0,1] interval, accounting for the particularities of circular variables (Camus et al., 2011). In particular, the values of circular variables were divided by π , while min-max normalization was applied to the remaining components. These sea states were propagated to the study sites using DELFT3D, from which wave data were obtained at depths of approximately 20-25 m. The transformed data for the selected climate states were then used to interpolate, using techniques based on radial basis functions (Hardy, 1971), the values of other climate states with different combinations of variables, enabling the reconstruction of the complete transformed series in the study area.

3.3.2 Estimation of water levels, discharges, and sediment supply at river mouths

River discharges, water levels, flood extents, and sediment supply to the coast were estimated using the Guadalfortran model. The model was driven by time series of river discharge and total sea level—composed of mean sea level and storm surge values—as a boundary condition applied at an offshore location near the river mouth. The methodology varies depending on data availability and the significance of each watercourse. For minor rivers and creeks with small and irregular runoff, the SCS-GDFA model (described in the SM) was implemented and fed with precipitation simulation time series to estimate catchment contributions to the main river course. For non-regulated rivers, data from E-HYPEcatch were directly used. In other cases, information on historical discharge management was considered to transform reservoir inflow into dam outflows. In the latter case, data were used to simulate the final 2 km of the river to obtain flood curves at the mouth. From river flow data, solid sediment supply was estimated for bedload and suspended sediment transport using the average of values obtained from the formulations of Bagnold (1966); Brownlie and Keck (1981); Meyer-Peter and Müller (1948) and Wilcock and Crowe (2003).

The outputs of this process, for each climate realization, are time series of waves and sea level, and, where applicable, river discharge and sediment supply at river mouths in the vicinity of each study section.

3.4 Simulation of hydro-morphodynamic processes

Waves, water level, and sediment supply data were used to simulate the temporal evolution of the coastline using the

CoastalME model, by sequentially reproducing hydromorphodynamic processes and associated morphological changes at a time step of 3 h. The coastline configuration for each time step was based on the output of the previous one.

Along this process, hydrodynamic conditions were recorded at a temporal resolution of three hours, while topobathymetric properties were saved monthly and at six-hour intervals during storm events and periods of high river discharge, with additional recordings at the onset and conclusion of each event. Maritime storm events were defined by a significant wave height threshold of 1.5 m, a minimum duration of 30 h, and a minimum inter-event interval of 24 h (Lira-Loarca et al., 2020). Fluvial discharge events were characterized by a threshold flow rate of 5 m³/s, which was found to be a suitable value for defining Poisson-type events whose sediment contributions were significant enough to be considered. To quantify the wave contribution to total water level, wave setup and runup were estimated using the empirical formulation of Stockdon et al. (2006), which integrates significant wave height, peak wave period, and beach slope to estimate the maximum waveinduced water level elevation. This integrated dataset captures both hydrodynamic forcing-including wave-induced water level variations—and the resulting topobathymetric changes, enabling a comprehensive and coupled assessment of coastal system response.

The results of this task consist of 20 equally likely realizations of dynamic random sets characterizing erosion and flooding in the subunits under a climate change scenario spanning 75 years, from the beginning of 2025 to the end of 2100.

3.5 Statistical characterization of erosion and flooding

Based on the evolution of topobathymetric data, the spatial and temporal variability of several random variables is analyzed for all beaches within each subunit. The NS treatment of climate enables analysis across different time scales, including monthly, seasonal (for peak and off-peak tourist periods, ranging from April 1st to September 30th for the peak tourist season and from October 1st to March 31st for the off-peak tourist season), and annual resolutions. In particular, the position of the mean sea level line is examined, defined as the intersection between the local mean sea level plane and the beach profile. A companion paper by Otiñar et al. (2025) presents a selection of these random variables, specifically defined to support decision-making in alignment with the Spanish legal framework.

4 Results

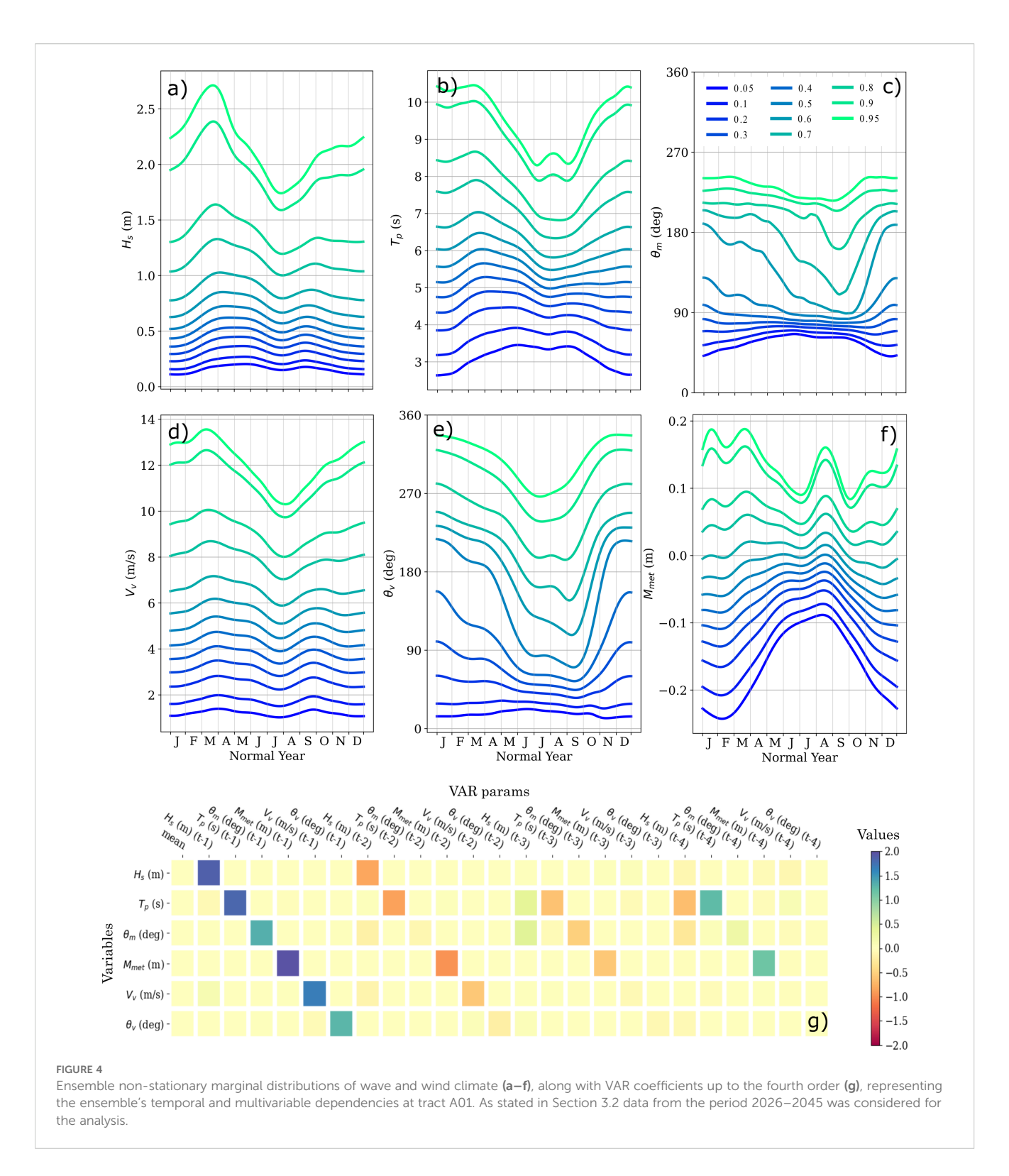
After summarizing the results of the physical environment characterization, we present the results for Subunit 1 of Tract 'A01' in Almería province, identified as 'A01-001'. In the companion paper by Otiñar et al. (2025), we also present overall results obtained along the analyzed coast. Within this subunit is

Guainos Beach, a semi-urban beach composed of dark gravel and sand, approximately 700 meters in length and 15 meters in width, with negligible tidal variation O(40 cm). The beach is bounded by a small rocky cliff to the west and a transverse breakwater to the east. It has three additional transverse breakwaters at its easternmost end. The Guainos River creek flows into the sea near the western end. Precipitation within the basin is scarce, with prolonged dry periods during the summer—typical of semiarid regions.

The characterization of the study area resulted in the identification of nine tracts—three in Granada and six in Almería—and a total of 67 subunits within them. Supplementary Table S3 lists these tracts and subunits, including a representative element for each subunit, as well as the characteristics of the computational meshes used in CoastalME. Figure 3 shows the delimitation of the tracts over physical maps of the provinces of Granada (A) and Almería (B), along with the location of wave, river discharge, and precipitation datasets, as well as other elements such as the coastline, river courses, basins, and reservoirs. A total of seven rivers and 30 minor watercourses were considered. The information is zoomed into panel (C), which focuses on subunit A01–001 and shows the initial position of the mean water level line.

4.1 Climate characterization by tract

Wave and wind analyses were conducted for each tract at the offshore locations indicated in Figure 3B. Figure 4 presents the results of the statistical characterization of the maritime climate ensemble projection in the vicinity of Guainos Beach. The non-stationary marginal compound distributions obtained for the variables H_S , T_p , θ_m , η_{met} , V_w and θ_w are shown in panels (a) to (f). Panel (g) displays the coefficients of the ensemble VAR model, which relates the current values at time t with those at the three preceding time steps (t-1, t-2, and t-3). Additional lags, up to t-78 h, are omitted for brevity. The climate analysis figures from which Figure 4 was derived are provided in Supplementary Figures S1-S7. The wave climate exhibits a clear seasonal pattern, with more severe conditions occurring between January and April, when maximum significant wave heights reach up to 2.5 m (panel a), wind speeds exceed 12 m/s (panel e), and storm surge approaches 0.15 m at the 99th percentile (panel d). The peak wave period (panel b) ranges between 3 and 11 seconds. Both the wave and wind climates display a bimodal directional pattern, with predominant directions from the second quadrant (80°/60°) and third quadrant (195°/225°) (panels c and f). Panel (g) of Figure 4 shows the typical diagonal bands in the VAR matrix, indicating stronger autoregressive relationships of each variable with its own past values. These relationships are clearly visible up to lag 2. Beyond this, H_S , V_w , and θ_w show a decrease in self-dependence, indicating a weakening of temporal correlation beyond three hours. In contrast, T_p , θ_m and η_{met} maintain their dependence up to lag 4, with a sharp decline thereafter. This panel also highlights the cross-variable influences-for example, how wave height affects the peak period and mean direction [see H_S (m) at t-3 and T_p (s) or θ_m (°)]. This



parameterization is specific to this location and differs from patterns observed in other models (see panel (g) of Supplementary Figures \$1_\$57)

Supplementary Figure S10 display the corresponding results related to precipitation characterization, with values ranging from 0 to 5 mm/h and extended dry periods observed during the summer months.

4.2 Transformation of climate states from tracts to subunits

Supplementary Figure S8 presents scatter plots of paired maritime variables, where all simulation points are shown as blue dots, and those corresponding to the representative climate states selected using the MDA algorithm are highlighted. These

representative states were transformed into study sites using DELFT3D, implementing over nine curvilinear grids (one per tract). The layout and spatial configuration of these grids, along with the corresponding bathymetry for the selected tract (A01), are shown in Supplementary Figure S9.

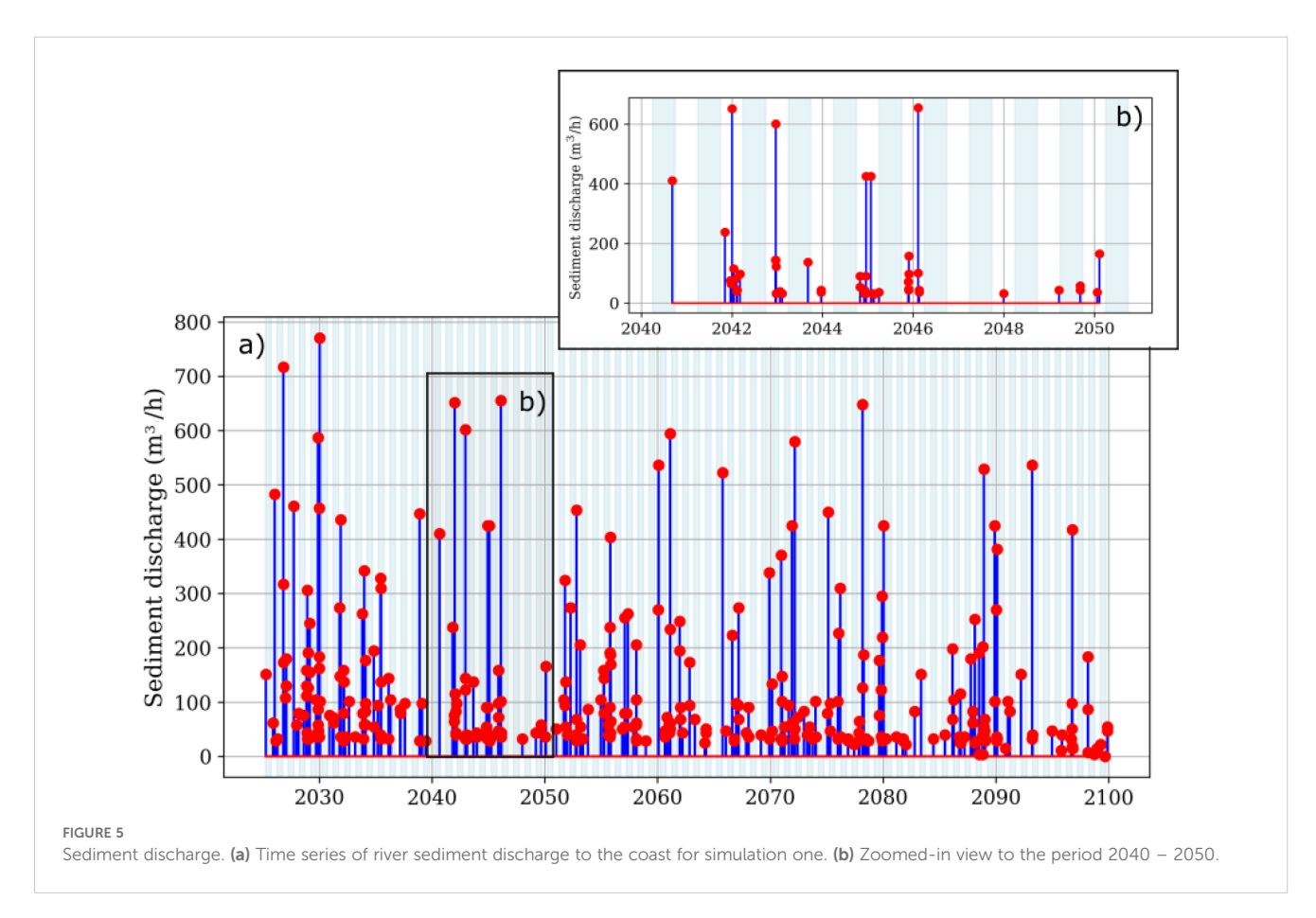
Regarding precipitation, the catchment's contribution to the watercourse was estimated using the SCS-GDFA model, incorporating the relative influence of precipitation data derived from the Thiessen polygons shown in Supplementary Figure S11. This figure depicts the Guainos Creek basin, the locations of available precipitation data points, and land use information within the catchment. Precipitation data from each model were statistically analyzed following the same methodology applied to the wave climate (see Supplementary Figure S10). Precipitation was simulated using the same approach as for the other variables and served as input for the SCS-GDFA model, which computes runoff. The resulting runoff was then used as input for the Guadalfortran model (see Section 4 of the SM). Figure 5 shows the resulting sediment discharge at the river mouth for a single simulation, as computed by Guadalfortran. Peak discharges reached up to 800 m³/ h, although only 10% of events exceeded 300 m³/h. A detailed view of the 2040-2050 period reveals that most discharge eventsincluding the most intense-occurred during the winter months or the low tourist season, reflecting the marked seasonality of precipitation in the region (see Supplementary Figure S10).

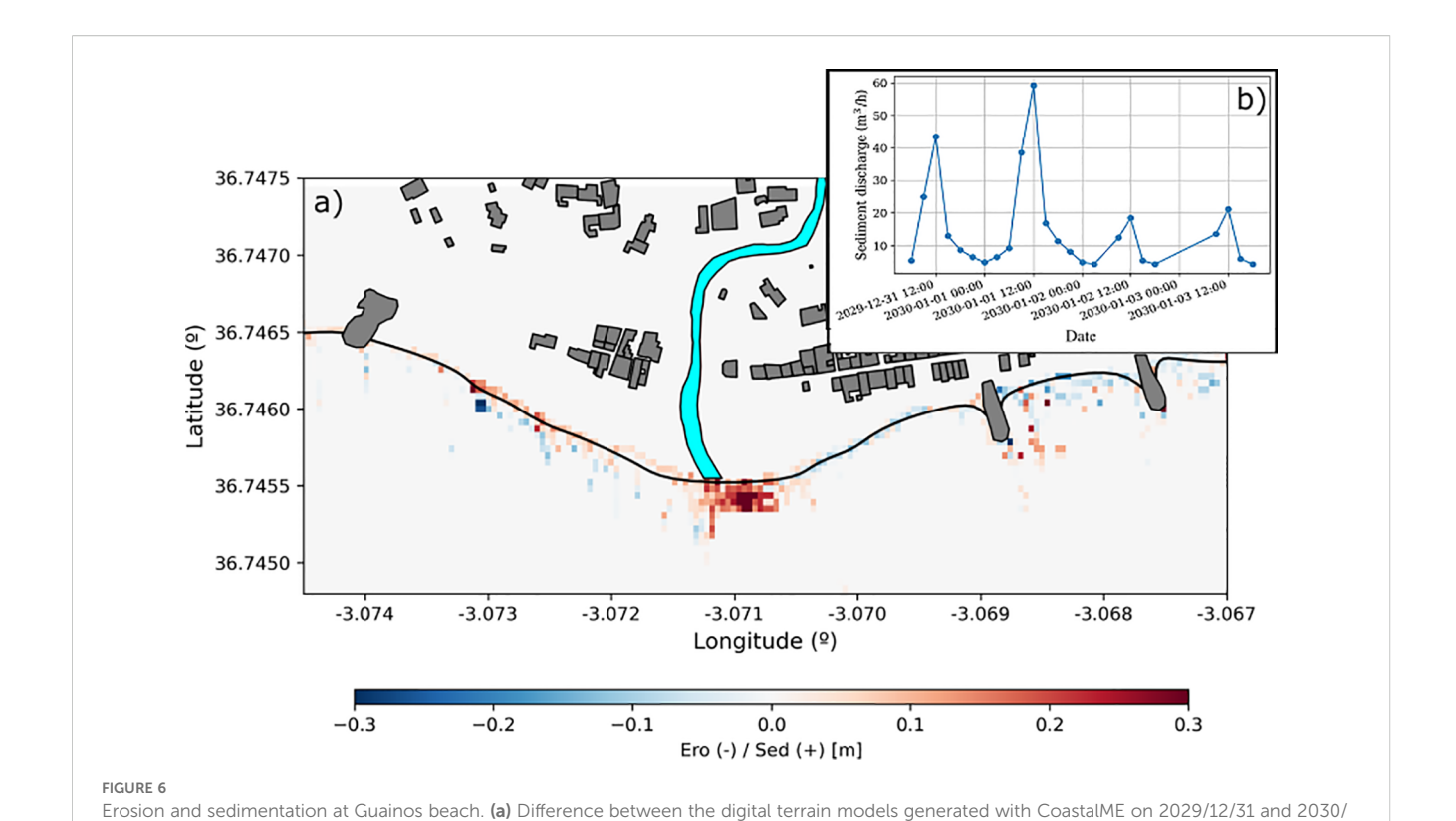
4.3 Simulation of hydro-morphodynamic processes

The outcome of the CoastalME simulation for subunit one is illustrated in Figure 6, which shows the difference between digital terrain models before and after a four-day period at the end of 2030. During this period, a multi-peak discharge event occurred under relatively high south-westerly wave conditions. The figure reveals that sediment supplied by the river is deposited to the east of the creek mouth. Erosion is observed in the deeper portion of the beach profile, while sediment accumulation occurs on the foreshore west of the mouth. On the lee side of the delta, eastward longshore drift causes widespread erosion and sand accumulation near the westernmost groin. Sand bypasses the tip of this structure and accumulates on the small beach located between the groins, which is predominantly subject to erosion.

4.4 Statistical characterization of erosion and flooding

Figure 7 shows several curves related to the mean sea level line at the end of t_H = 2030, 2050, and 2099. Specifically, it displays the 50% probability curve (solid line), along with the boundaries of the zone within which the line is expected to lie with 90% probability.





01/04, before and after a river discharge event in simulation one. The thick black solid line represents the initial mean sea level contour. Grey-filled polygons indicate buildings, structures, or rocky cliffs, while the main channel of the river creek is shown in light blue. (b) Illustration of the sediment

These boundaries correspond to the 5% and 95% probability isolines (dashed blue and red lines, respectively). In this context, the probability at a point on the beach refers to the likelihood of it being seaward of the mean sea level line. At $t_H = 2030$ (Figure 7A), the entire region exhibits erosion. Some simulations indicate sediment accumulation at the river mouth and near the groins, as shown by the dashed red line. Episodic river discharges contribute to the development of an incipient delta lobe at the creek mouth, which advances approximately 10 meters by 2050 (Figure 7B) and 20 meters by 2100 (Figure 7C), while migrating about 20 meters eastward by the end of the century. Coastal retreat is particularly pronounced on the western side of the delta, where it reaches an average of 25 meters by 2099, with differences of up to 15 meters

discharge during the stormy period.

between the 5% and 95% probability curves.

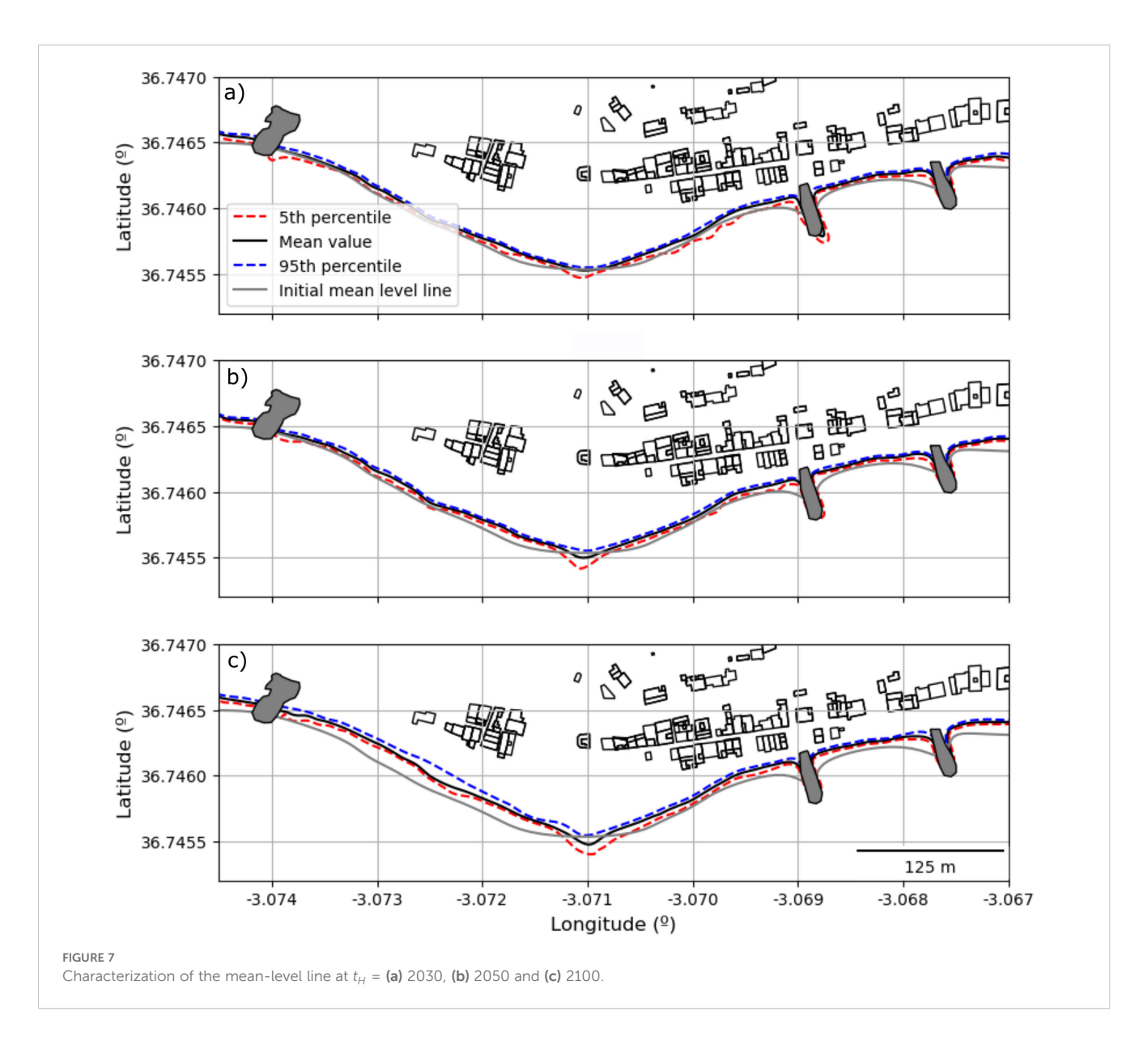
This temporal variability is also illustrated in Figure 8, which shows the mean variation in total area relative to the mean shoreline position at the start of the simulation, along with the 5th and 95th percentiles. The graph also includes the results from the 20 simulations. Panel (A) represents the entire simulation period, while panel (B) provides a zoomed-in view highlighting more detailed observations of the magnitude of changes during the summer and winter seasons. On average, there is a net loss of beach area. Until 2045, the probability of a net increase in area is not negligible, as indicated by the positive values of the 5th percentile. Superimposed on the main trend is a seasonal variation linked to the non-stationary treatment of the wave climate. Due to the decision to use the wave climate from 2026 to 2045 as representative of the entire

century, as explained in Section 3.2, the impact of wave conditions may be overshadowed by the rise in sea levels. This last point is also supported by the noticeable jump in the time series around the year 2080, when SLR approaches 50 cm. This behavior is associated with the increased frequency with which the total sea level reaches and surpasses the berm. Indeed, along the beach sector to the west of the river mouth, the berm is currently approximately 1 m above today's mean sea level, and the more frequent action of waves over a higher sea level triggers a more rapid progression of erosion.

The interannual variability of compound flooding is illustrated in Figure 9, which shows the probability of flooding for each month at the time horizon $t_H = 2100$. From June to September, the final stretch of the river and its mouth are unlikely to experience flooding (with probabilities smaller than 20%), while during the winter months, the probabilities increase, reaching up to 50%.

5 Discussion and concluding remarks

We have presented a methodology developed within the ICCOAST project for making joint projections of erosion and flooding due to the combined action of maritime and riverine forcings under the RCP 8.5 climate pathway. To the best of the authors' knowledge, this is the first work that explicitly considers sediment supply from watercourses, geological setting, the presence of obstacles, and climate non-stationarity. The methodology is applicable to a variety of coastal typologies, including deltaic

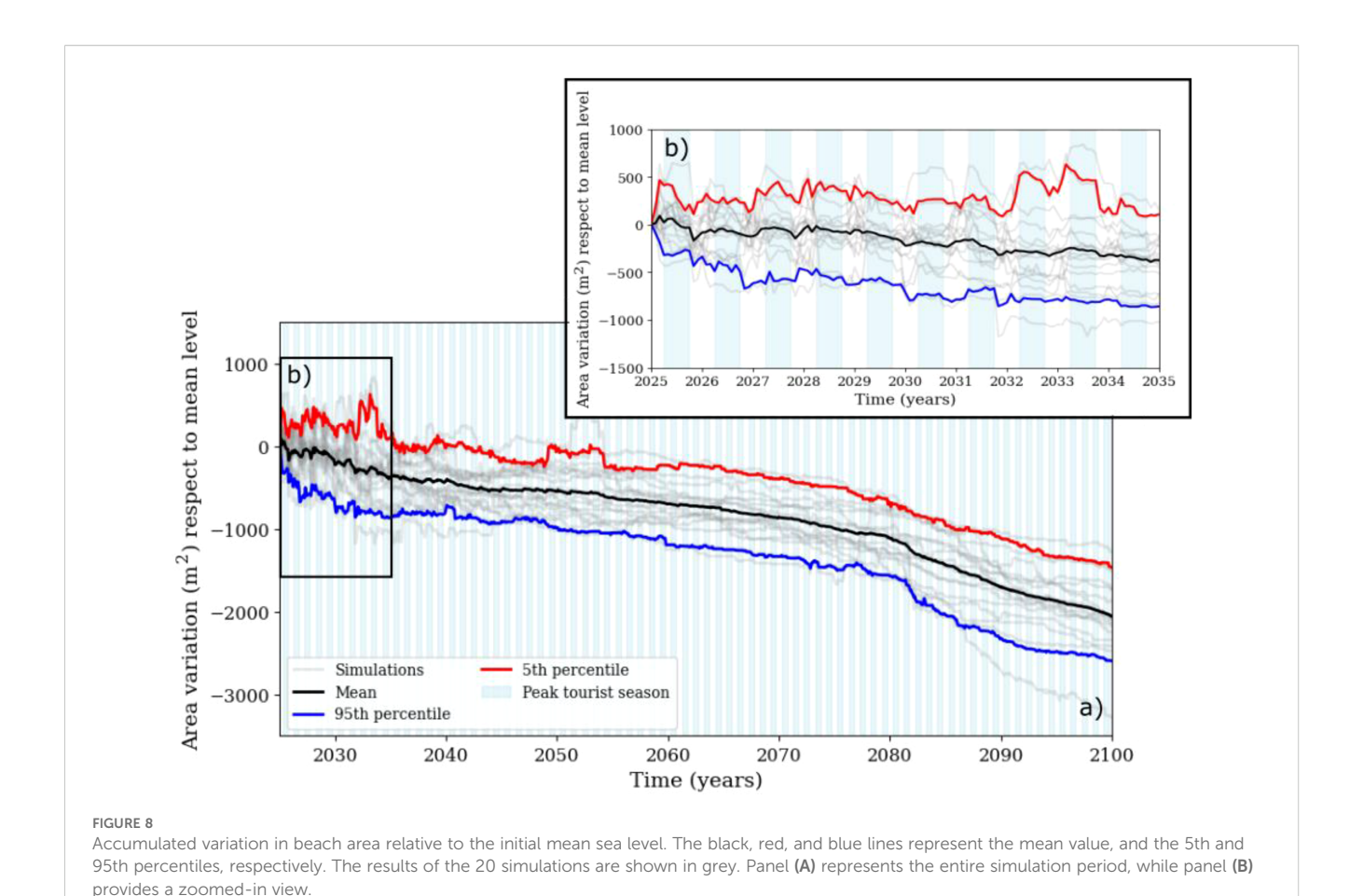


systems, natural pocket beaches, headland bay beaches, and other coastal landforms developed in the shelter of marine structures. Moreover, as discussed in detail in a companion paper by Otiñar et al. (2025), it allows for the assessment of the intrinsic uncertainty of a collection of random sets that can be tailored to the management requirements of the analysis.

As mentioned in Section 3.2, future climate is addressed through a multivariate, non-stationary, multi-model ensemble characterization (Lira-Loarca et al., 2021), which applies a Bayesian approach to marginal distributions to account for uncertainty regarding the true state of nature. The non-stationary framework, together with the inclusion of riverine forcings, enables the analysis of the spatiotemporal variability of flooding driven by both maritime climate and episodic river discharge events typical of arid and semi-arid Mediterranean coastal stretches. Additionally, this non-stationary treatment of climate forcings allows results to be distinguished across different time scales—such as monthly or touristic seasons—associated with annual climate variability. This seasonal analysis reveals significant

differences between peak and off-peak seasons, enabling authorities to make informed decisions regarding authorizations for the use and occupation of the coastal zone. The choice of one year as the reference time unit in the non-stationary climate characterization and simulation is due to the limited length of available climate projections (20 years for wave climate), which prevents analysis at longer climate variability scales (Cobos et al., 2022c; Lira-Loarca et al., 2021), such as the 11-year Schwabe cycle or the 22-year cycle (Usoskin et al., 2004), both linked to solar activity and associated with major climate indices.

As also noted in Section 3.2, due to the unavailability of precipitation projections from the models used for wave and wind, the random variables representing river discharge and precipitation were assumed to be independent of the other variables. This assumption is justified by the semi-arid to arid nature of the river basins in the study area, where fluvial discharges are rare events typically decoupled from wind-wave storms (Losada et al., 2011). However, when this is not the case, a joint analysis is recommended. Given the large spatial scope of the ICCOAST methodology (over 1,000 km of the Andalusian coast),

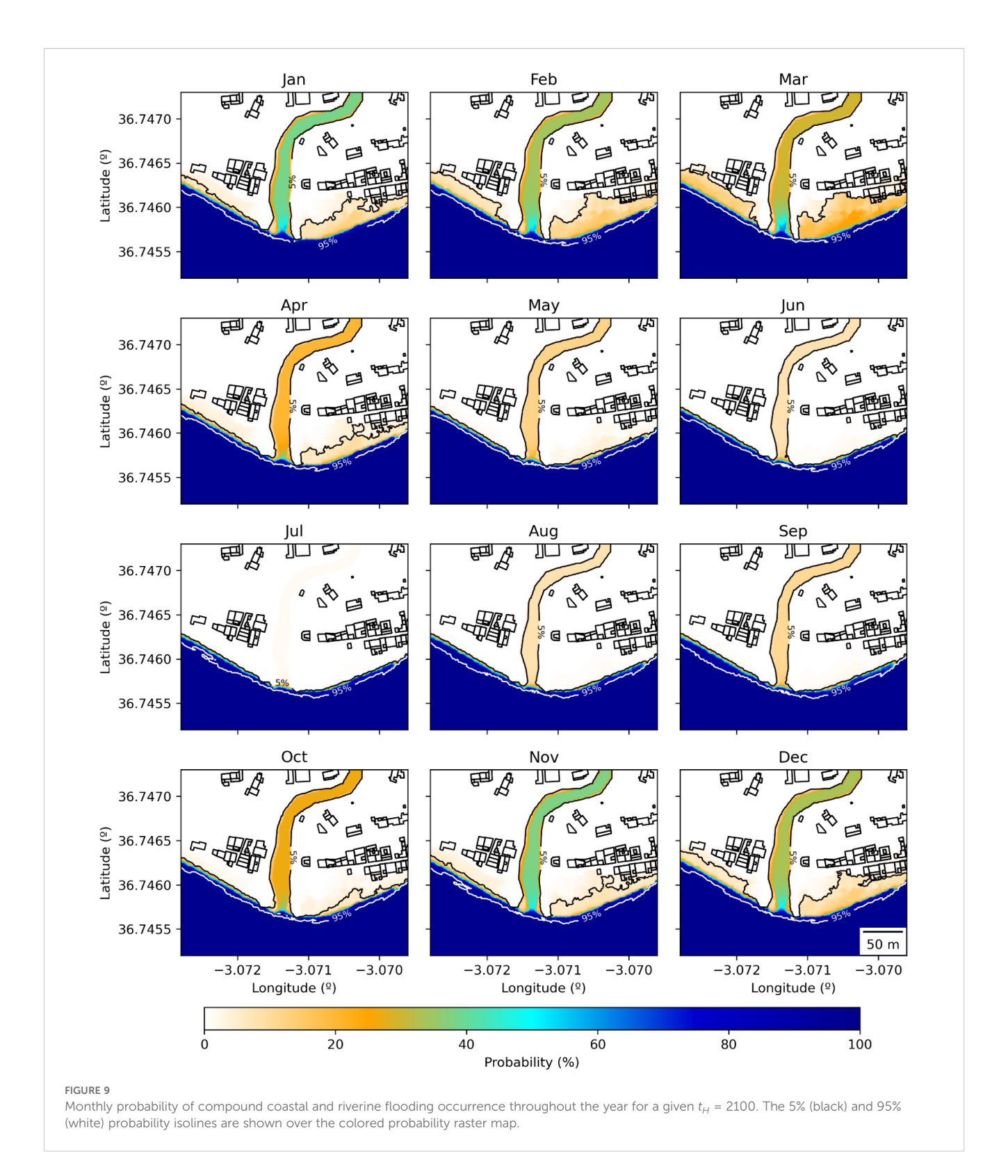


several simplifications have been made. First, the methodology decouples hydrodynamic and morphodynamic processes by keeping the seabed constant during each sea state. This assumption, based on the differing temporal scales of hydrodynamic and morphodynamic responses, is valid for short- to medium-term analyses, but does not capture the non-linear behavior of coastal systems over the long term (De Vriend et al., 1993). Additionally, a simplified morphological model is employed in which cross-shore processes are not considered. This approach assumes equilibrium beach profiles and treats cross-shore sediment transport as a perturbation superimposed on long-term coastal change (Payo et al., 2017). On the Mediterranean Andalusian coast-where the wave climate features nearly opposing dominant directions (Losada et al., 2011), typically approaching obliquelyalongshore sediment transport governs the sediment budget (see, e.g., Fredsoe and Deigaard (1992)). However, cross-shore transport may play a critical role in short-term changes, particularly during storm events and post-storm recovery (Bergillos et al., 2017), and may interact with alongshore transport. Despite the simplifications made, the methodology offers the advantage of being modular, allowing any of its components to be modified or enhanced to incorporate additional processes or to tailor the analysis to specific coastal stretches.

Regarding SLR, the model does not explicitly incorporate the socalled Bruun effect (Bruun, 1954; 1962), unlike other studies such as Álvarez-Cuesta et al. (2021a) and Toimil et al. (2021, 2023), which apply the original Bruun formulation. This formulation has been questioned due to challenges in estimating its parameters and concerns about its applicability beyond its originally intended context. Although alternative formulations have been proposed to address these limitations and extend their applicability (e.g., Dean and Houston, 2016; Dean and Maurmeyer, 2018; Edelman, 1969; Rosati et al., 2013), they are often based on site-specific field data and are not directly transferable to beaches with different characteristics. The approach presented here is more closely aligned with that of Ranasinghe et al. (2012), which uses synthetic climate and sea level data to force a morphological model.

In this study, a single time series corresponding to the ensemble mean of 20 GCMs is used to represent SLR. This contrasts with the approach of Álvarez-Cuesta et al. (2021b) and Toimil et al. (2021, 2023), which employ multiple SLR time series from different percentiles, treating the resulting outcomes as equally probable to reduce uncertainty. An alternative approach—not pursued here due to computational constraints—would be to present results under multiple SLR scenarios, in the style of a scenario-based analysis.

Compound flooding is addressed by integrating maritime and fluvial dynamics using two coupled numerical models. The sea level is set as the downstream boundary condition in the Guadalfortran model that simulates the river's hydrodynamics, to achieve this coupling. This sea level incorporates contributions from the mean sea level, as well as from astronomical and meteorological tides. Consequently, water levels throughout the river channel are influenced by river discharge and maritime forcing. However, this approach neglects the effect of river discharge on the water levels of adjacent beaches. The level prescribed



to the Guadalfortran model at the river mouth is also used as input in the CSHORE model, which simulates maritime hydrodynamics within the CoastalME model.

The resulting inundation domains, one from the fluvial model and one from the coastal evolution model, are represented in raster format and combined spatially to define the total flood extent. This modular

coupling strategy allows processes to be integrated in a practical way, while ensuring that computational costs remain manageable.

Several simplifications have been made within this framework. Firstly, the seabed topography within the river channel is assumed to remain constant throughout the simulation. Secondly, the sea level is kept fixed for each three-hour sea state, in line with the wave climate

input. While this assumption is suitable for capturing general patterns, it may overlook short-term nonlinear interactions between river discharge and maritime forcing. These interactions can be associated with rapidly evolving storm conditions or the interplay between tides, surges and waves, which operate at finer temporal scales. These limitations are well documented in the literature on compound flooding, where a lack of finer temporal resolution can lead to the underestimation of the impact of critical peaks (e.g. Moftakhari et al., 2017; Bilskie and Hagen, 2018). For this reason, this approximation may only be reasonably valid for small rivers with low discharge and microtidal environments, where the influence of riverine flows on sea level is minimal and the effect of waves within the river mouth is negligible.

The analysis of the variation in mean shoreline position is illustrated with results from Guainos Beach, where a net loss of beach area is observed on average. Superimposed on this general trend is a clear seasonal variation, attributed to the non-stationary treatment of climate. This seasonal variation is more pronounced during the first 15 years; thereafter, the influence of wave climate conditions gradually diminishes, and the trend appears to be primarily driven by SLR. Although this behavior could be partly attributed to the use of constant wave climate conditions derived from the 2026–2045 period (due to data gaps in wave projections), the lack of significant differences in wave climate compared to the later available period (2081–2100) suggests a progressive increase in the relative importance of SLR. Results regarding the compound flooding shows a strong variability of probability of flooding across months particularly at the final stretch of the river and its mouth.

Although there are no specific studies on the historical evolution or future projections of the variables analyzed in this article for Guainos beach, the companion paper (Otiñar et al., 2025) presents results based on multiple random sets for this beach and the wider coastal areas of Granada and Málaga. The future projections in that analysis are consistent with previously documented trends along the Andalusian coast, particularly regarding the spatial distribution of the most critical sectors and the expected intensity of impacts. Specifically, the identification of areas prone to erosion and flooding, as well as the magnitude of projected shoreline retreat, aligns with historical patterns observed by Prieto Campos and Ojeda Zújar (2024) in the provinces of Granada and Almería, based on shoreline evolution from 2001 to 2019. The agreement between these historical trends and the future projections, despite the different time periods and methods involved, supports the robustness of the modelling approach and strengthens confidence in the projections presented for the 21st century (2025–2100).

Data availability statement

The raw data supporting the conclusions of this article will be made available by the authors, without undue reservation.

Author contributions

PO: Data curation, Investigation, Methodology, Validation, Writing – review & editing, Software, Visualization, Formal analysis, Writing – original draft. MC: Formal analysis, Investigation, Software, Validation, Writing – review & editing, Supervision, Methodology. MS: Investigation, Data curation, Validation, Writing – original draft,

Software. AM: Methodology, Writing – review & editing. AB: Project administration, Funding acquisition, Conceptualization, Supervision, Writing – original draft, Investigation, Writing – review & editing.

Funding

The author(s) declare financial support was received for the research and/or publication of this article. This work was funded by Junta de Andalucía – Consejería de Universidad, Investigación e Innovación – Proyecto (Ref. ProyExcel_00375, EPICOS). The work was conducted within the framework of contracts (Exped. Contr. 2018–66984 and 2020-687686) that were competitively bid by the Junta de Andalucía (with funds of the Fondo Europeo de Desarrollo Regional) and awarded to the University of Granada (Lot I). MC is indebted to Consejería de Transformación Económica, Industria, Conocimiento y Universidades de la Junta de Andalucía (POSTDOC_21_00724) which partially funded his work.

Conflict of interest

The authors declare that the research was conducted in the absence of any commercial or financial relationships that could be construed as a potential conflict of interest.

Correction note

This article has been corrected with minor changes. These changes do not impact the scientific content of the article.

Generative AI statement

The author(s) declare that no Generative AI was used in the creation of this manuscript.

Any alternative text (alt text) provided alongside figures in this article has been generated by Frontiers with the support of artificial intelligence and reasonable efforts have been made to ensure accuracy, including review by the authors wherever possible. If you identify any issues, please contact us.

Publisher's note

All claims expressed in this article are solely those of the authors and do not necessarily represent those of their affiliated organizations, or those of the publisher, the editors and the reviewers. Any product that may be evaluated in this article, or claim that may be made by its manufacturer, is not guaranteed or endorsed by the publisher.

Supplementary material

The Supplementary Material for this article can be found online at: https://www.frontiersin.org/articles/10.3389/fmars.2025.1631041/full#supplementary-material

References

Álvarez-Cuesta, M., Toimil, A., and Losada, I. J. (2021a). Modelling long-term shoreline evolution in highly anthropized coastal areas. Part 2: Assessing the response to climate change. *Coast. Eng.* 168. doi: 10.1016/j.coastaleng.2021.103961

Álvarez-Cuesta, M., Toimil, A., and Losada, I. J. (2021b). Modelling long-term shoreline evolution in highly anthropized coastal areas. Part 1: Model description and validation. *Coast. Eng.* 169. doi: 10.1016/j.coastaleng.2021.103960

Ávila, A. (2007). Procesos de múltiple escala en la evolución de la línea de costa. PhD Thesis in Spanish (Spain: Universidad de Granada), 161.

Ávila, A. (2008). Modelo Unidimensional de Flujo no Estacionario en Cauces Naturales - Guadalfortran (43g).

Bagnold, R. (1966). "An approach to the sediment transport problem from general physics," in *Geological Survey Professional Papel 422*. (Washington, D.C.: U.S. Government Printing Office).

Baquerizo, A., and Losada, M. A. (2008). Human interaction with large scale coastal morphological evolution. An assessment of the uncertainty. *Coast. Eng.* 55, 569–580. doi: 10.1016/j.coastaleng.2007.10.004

Bergillos, R. J., Masselink, G., and Ortega-Sánchez, M. (2017). Coupling cross-shore and longshore sediment transport to model storm response along a mixed sand-gravel coast under varying wave directions. *Coast. Eng.* 129, 93–104. doi: 10.1016/j.coastaleng.2017.09.009

Bilskie, M. V., and Hagen, S. C. (2018). Defining flood zone transitions in low-gradient coastal regions. *Geophys. Res. Lett.* 45, 2761–2770. doi: 10.1002/2018GL077524

Booij, N., Ris, R. C., and Holthuijsen, L. H. (1999). A third-generation wave model for coastal regions 1. Model description and validation. *J. Geophys. Res.: Oceans.* 104, 7649–7666. doi: 10.1029/98JC02622

Brownlie, W. R., and Keck, W. M. (1981). Compilation of alluvial channel data: Laboratory and field. (Pasadena, California: W.M. Keck Laboratory, Caltech).

Bruun, P. (1954). Coastal erosion and development of beach profile Vol. Vol. 44 (US Beach Erosion Board).

Bruun, P. (1962). Bruun - 1962 - Engineering Aspects of Sediment Transport. (Gainesville, Florida: Florida Engineering and Industrial Experiment Station).

Callaghan, D. P., Nielsen, P., Short, A., and Ranasinghe, R. (2008). Statistical simulation of wave climate and extreme beach erosion. *Coast. Eng.* 55, 375–390. doi: 10.1016/j.coastaleng.2007.12.003

Camus, P., Mendez, F. J., Medina, R., and Cofiño, A. S. (2011). Analysis of clustering and selection algorithms for the study of multivariate wave climate. *Coast. Eng.* 58, 453–462. doi: 10.1016/j.coastaleng.2011.02.003

Cantalejo, M., Cobos, M., Millares, A., and Baquerizo, A. (2024). A non-stationary bias adjustment method for improving the inter-annual variability and persistence of projected precipitation. *Sci. Rep.* 14, 25923. doi: 10.1038/s41598-024-76848-2

Caretta, M. A., Mukherji, A., Arfanuzzaman, M., Betts, R. A., Gelfan, A., Hirabayashi, Y., et al. (2022). "Water," in Climate Change 2022: Impacts, Adaptation and Vulnerability. Contribution of Working Group II to the Sixth Assessment Report of the Intergovernmental Panel on Climate Change. Eds. H.-O. Pörtner, D. C. Roberts, M. Tignor, E. S. Poloczanska, K. Mintenbeck, A. Alegría, M. Craig, S. Langsdorf, S. Löschke, V. Möller, A. Okem and B. Rama (Cambridge University Press, Cambridge, UK and New York, NY, USA), 551–712. doi: 10.1017/9781009325844.006

Cobos, M., Otiñar, P., Magaña, P., and Baquerizo, A. (2022c). A method to characterize climate, Earth or environmental vector random processes. *Stochastic. Environ. Res. Risk Assess.* 36, 4073–4085. doi: 10.1007/s00477-022-02260-9

Cobos, M., Otiñar, P., Magaña, P., Lira-Loarca, A., and Baquerizo, A. (2022b). MarineTools.temporal: A Python package to simulate Earth and environmental time series. *Environ. Model. Software.* 150. doi: 10.1016/j.envsoft.2022.105359

Cobos, M., Payo, A., Favis-Mortlock, D., Burke, H. F., Morgan, D., Jenkins, G., et al. (2022a). "Importance of shallow subsurface and built environment characterization on assessing coastal landscape morphological evolution from hours to decadal time scales: application to complex landforms along andalucía (Spain) coastline," in *Proceedings of the 39th IAHR World Congress*.

Cooley, S., Schoeman, D., Bopp, L., Boyd, P., Donner, S., Ghebrehiwet, D. Y., et al. (2022). "Oceans and coastal ecosystems and their services," in Climate Change 2022: Impacts, Adaptation and Vulnerability. Contribution of Working Group II to the Sixth Assessment Report of the Intergovernmental Panel on Climate Change. Eds. H.-O. Pörtner, D. C. Roberts, M. Tignor, E. S. Poloczanska, K. Mintenbeck, A. Alegria, M. Craig, S. Langsdorf, S. Löschke, V. Möller, A. Okem and B. Rama (Cambridge University Press, Cambridge, UK and New York, NY, USA), 379–550. doi: 10.1017/9781009325844.005

Cowell, P. J., Stive, M. J., Niedoroda, A. W., de Vriend, H. J., Swift, D. J., Kaminsky, G. M., et al (2003). The coastal-tract (part 1): a conceptual approach to aggregated modeling of low-order coastal change. *J. Coastal Res.* 812–827.

d'Anna, M. (2022).). Modelling past and future sandy shoreline change and the respective uncertainties: toward a holistic approach (Université de Bordeaux).

Davidson, M. A., Lewis, R. P., and Turner, I. L. (2010). Forecasting seasonal to multi-year shoreline change. *Coast. Eng.* 57, 620–629. doi: 10.1016/j.coastaleng.2010.02.001

Dean, R. G., and Houston, J. R. (2016). Determining shoreline response to sea level rise. *Coast. Eng.* 114, 1–8. doi: 10.1016/j.coastaleng.2016.03.009

Dean, R. G., and Maurmeyer, E. M (2018). "Models for beach profile response," in *Handbook of Coastal Processes and Erosion*. Eds. P. Komar and J. R Moore. [Boca Raton, Florida: CRC Press (Taylor & Francis Group)].

Deltares (2014). *Delft3D Suite (Version 4.00)* (4.0.0) (Deltares). Available online at: https://www.deltares.nl/en/software-and-data/products/delft3d-4-suite/ (Accessed August 16, 2025).

Déqué, M., Rowell, D. P., Lüthi, D., Giorgi, F., Christensen, J. H., Rockel, B., et al. (2007). An intercomparison of regional climate simulations for Europe: Assessing uncertainties in model projections. *Clim. Change* 81, 53–70. doi: 10.1007/s10584-006-9278_x

De Vriend, H. J., Capobianco, M., Chesher, T., De Swart, H. E., Latteux, B., and Stive, M. J. F. (1993). Approaches to long-term modelling of coastal morphology: a review. *Coast. Eng.* 21, 225–269. doi: 10.1016/0378-3839(93)90051-9

Ding, Y., Kim, S. C., Frey, A. E., Permenter, R. L., and Styles, R. (2018). "Probabilistic modeling of long-term shoreline changes in response to sea level rise and waves," in *Scour and Erosion IX, Proceedings of ICSE*. 203–211.

Donnelly, C., Andersson, J. C. M., and Arheimer, B. (2016). Using flow signatures and catchment similarities to evaluate the E-HYPE multi-basin model across Europe. *Hydrolog. Sci. J.* 61 (2), 255–273. doi: 10.1080/02626667.2015.1027710

Edelman, T. (1969). "Dune erosion during storm conditions," in *Coastal Engineering*. (Delft. Países Bajos: Delft Hydraulics Laboratory), 719–722.

Fox-Kemper, B., Hewitt, H. T., Xiao, C., Aðalgeirsdóttir, G., Drijfhout, S. S., Edwards, T. L., et al. (2021). "Ocean, cryosphere and sea level change," in *In Climate Change 2021: The Physical Science Basis. Contribution of Working Group I to the Sixth Assessment Report of the Intergovernmental Panel on Climate Change.* Eds. V. Masson-Delmotte, P. Zhai, A. Pirani, S. L. Connors, C. Péan, S. Berger, N. Caud, Y. Chen, L. Goldfarb, M. I. Gomis, M. Huang, K. Leitzell, E. Lonnoy, J. B. R. Matthews, T. K. Maycock, T. Waterfield, O. Yelekçi, R. Yu and B. Zhou (Cambridge University Press, Cambridge, United Kingdom and New York, NY, USA), 1211–1362. doi: 10.1017/9781009157896.011

Fredsoe, J., and Deigaard, R. (1992). Mechanics of Coastal Sediment Transport. World Scientific. (Singapore: World Scientific Publishing Company).

Hardy, R. L. (1971). Multiquadric equations of topography and other irregular surfaces. J. Geophys. Res. 76, 1905–1915. doi: 10.1029/jb076i008p01905

Kennard, R. W., and Stone, L. A. (1969). Computer aided design of experiments. Technometrics 11, 137–148. doi: 10.1080/00401706.1969.10490666

Kobayashi, N. (2016). Coastal sediment transport modeling for engineering applications. *J. Waterway. Port. Coastal. Ocean. Eng.* 142. doi: 10.1061/(asce) ww.1943-5460.0000347

Kumar, S., and Vijay, P. (2003). Soil Conservation Service Curve Number (SCS-CN) Methodology Vol. 42 (Water Science and Technology Library).

Lesser, G. R., Roelvink, J. A., van Kester, J. A. T. M., and Stelling, G. S. (2004). Development and validation of a three-dimensional morphological model. *Coast. Eng.* 51, 883–915. doi: 10.1016/j.coastaleng.2004.07.014

Lira-Loarca, A., Cobos, M., Besio, G., and Baquerizo, A. (2021). Projected wave climate temporal variability due to climate change. *Stochastic. Environ. Res. Risk Assess.* 35, 1741–1757. doi: 10.1007/s00477-020-01946-2

Lira-Loarca, A., Cobos, M., Losada, M. Á., and Baquerizo, A. (2020). Storm characterization and simulation for damage evolution models of maritime structures. *Coast. Eng.* 156. doi: 10.1016/j.coastaleng.2019.103620

Losada, M. A. (2001). ROM 0.0 Procedimiento general y bases de cálculo en el proyecto de obras marítimas y portuarias. (Madrid, España: Puertos del Estado).

Losada, M. A. (2009). ROM 1.0-09 Recomendaciones del diseño y ejecución de las Obras de Abrigo (Parte 1ª. Bases y Factores para el proyecto. Agentes climáticos). (Madrid, España: Puertos del Estado).

Losada, M. A., Baquerizo, A., Ortega-Sánchez, M., and Ávila, A. (2011). Coastal evolution, sea level, and assessment of intrinsic uncertainty. *J. Coast. Res.* SPEC. ISSUE 59, 218–228. doi: 10.2112/SI59-023.1

Losada, M. A., Ortega-Sánchez, M., Baquerizo, A., and Santiago, J. M. (2008). Los cambios de morfología en la Costa Andaluza. (Sevilla, España: Junta de Andalucía, Conseiería de Medio Ambiente).

Magaña, P., Del-Rosal-Salido, J., Cobos, M., Lira-Loarca, A., and Ortega-Sánchez, M. (2020). Approaching software engineering for marine sciences: A single development process for multiple end-user applications. *J. Mar. Sci. Eng.* 8. doi: 10.3390/IMSE8050350

Magaña, P., Otiñar, P., Silva-Santana, M., Cobos, M., and Baquerizo, A. (2022). "Google Earth Engine-based detection of shoreline on mixed sand and gravel beaches," in *Proceedings of the 39th IAHR World Congress*. doi: 10.3850/IAHR-39WC2521711920221628

Mateos, R. M., López-Vinielles, J., Poyiadji, E., Tsagkas, D., Sheehy, M., Hadjicharalambous, K., et al. (2020a). Integration of landslide hazard into urban planning across Europe. *Landscape Urban. Plann.* 196. doi: 10.1016/j.landurbplan.2019.103740

Mateos, R. M., Sarro, R., Reyes-Carmona, C., Peña, E., Díez, A., Pérez, R., et al. (2020b). Los peligros geológicos en España y su gestión. Ejercicio participativo. [Madrid, España: Instituto Geológico y Minero de España (IGME)]. doi: 10.13140/RG.2.2.11801.44647

Meyer-Peter, E., and Müller, R. (1948). Formulas for bed-load transport. IAHSR 2nd Meeting, Appendix 2. [Delft, Países Bajos: IAHR (International Association for Hydraulic Research)].

Michelangeli, P. A., Vrac, M., and Loukos, H. (2009). Probabilistic downscaling approaches: Application to wind cumulative distribution functions. *Geophys. Res. Lett.* 36. doi: 10.1029/2009GL038401

Millares, A., Polo, M. J., Moñino, A., Herrero, J., and Losada, M. A. (2014). Bedload dynamics and associated snowmelt influence in mountainous and semiarid alluvial rivers. *Geomorphology* 206, 330–342. doi: 10.1016/j.geomorph.2013.09.038

Moftakhari, H. R., Salvadori, G., AghaKouchak, A., Sanders, B. F., and Matthew, R. A. (2017). Compounding effects of sea level rise and fluvial flooding. *Proc. Natl. Acad. Sci.* 114, 9785–9790. doi: 10.1073/pnas.1620325114

Otiñar, P., Cobos, M., Silva, M., and Baquerizo, A. (2025). Statistical characterization of projected flooding and erosion processes for coastal management. *Front. Mar. Sci.* 12. doi: 10.3389/fmars.2025.1631047

Panzeri, M., Stripling, S., and Chesher, T. (2012). "A GIS framework for probabilistic modelling of coastal erosion and flood risk," in *Proceedings of PIANC COPEDEC VIII*. Wallingford, UK: HR Wallingford Ltd.

Payo, A., Baquerizo, A., and Losada, M. (2003). Procedimiento para la simulación por estados de la evolución de la línea de playa a gran escala. *J. Españolas. Ingeniería. Costas. y. Puertos.* (Cádiz, Spain: Puerto de Santa María).

Payo, A., Baquerizo, A., and Losada, M. (2004). Cuantificando la incertidumbre: Aplicación a la línea de playa. *Ingeniería. Del. Agua.* 11, 211–220. doi: 10.4995/ia.2004.2529

Payo, A., Baquerizo, A., and Losada, M. (2008). Uncertainty assessment: Application to the shoreline. *J. Hydraulic. Res.* 46, 96–104. doi: 10.1080/00221686.2008.9521944

Payo, A., Favis-Mortlock, D., Dickson, M., Hall, J. W., Hurst, M. D., Walkden, M. J. A., et al. (2017). Coastal Modelling Environment version 1.0: A framework for integrating landform-specific component models in order to simulate decadal to centennial morphological changes on complex coasts. *Geosci. Model. Dev.* 10, 2715–2740. doi: 10.5194/gmd-10-2715-2017

Prieto Campos, A., and Ojeda Zújar, J. (2024). Methodology of data generation and calculation of erosion rates applied to littoral areas: Evolution of the Andalusian shoreline on exposed beaches during the 21st century, (2001-2019). *Invest. Geográficas*. 81), 9–31. doi: 10.14198/INGEO.25242

Ramírez, M., Menéndez, M., Paula, G., Braña, C., Losada Rodríguez, I. J., Lobeto, H., et al. (2019). Elaboración de la metodología y bases de datos para la proyección de impactos de cambio climático a lo largo de la costa española. (Logroño, España: Fundación Dialnet / Universidad de La Rioja).

Ranasinghe, R. (2016). Assessing climate change impacts on open sandy coasts: A review. Earth-Sci. Rev. 160, 320–332. doi: 10.1016/j.earscirev.2016.07.011

Ranasinghe, R., Callaghan, D., and Stive, M. J. F. (2012). Estimating coastal recession due to sea level rise: Beyond the Bruun rule. *Clim. Change* 110, 561–574. doi: 10.1007/s10584-011-0107-8

Ranasinghe, R., Ruane, A. C., Vautard, R., Arnell, N., Coppola, E., Cruz, F. A., et al. (2021). "Climate change information for regional impact and for risk assessment," in Climate Change 2021: The Physical Science Basis. Contribution of Working Group 1 to the Sixth Assessment Report of the Intergovernmental Panel on Climate Change. Eds. V. Masson-Delmotte, P. Zhai, A. Pirani, S. L. Connors, C. Péan, S. Berger, N. Caud, Y. Chen, L. Goldfarb, M. I. Gomis, M. Huang, K. Leitzell, E. Lonnoy, J. B. R. Matthews, T. K. Maycock, T. Waterfield, O. Yelekçi, R. Yu and B. Zhou (Cambridge University Press, Cambridge, United Kingdom and New York, NY, USA), 1767–1926. doi: 10.1017/9781009157896.014

Reeve, D. E., and Spivack, M. (2004). Evolution of shoreline position moments. Coast. Eng. 51, 661–673. doi: 10.1016/j.coastaleng.2004.07.002

Rosati, J. D., Dean, R. G., and Walton, T. L. (2013). The modified Bruun Rule extended for landward transport. *Mar. Geol.* 340, 71–81. doi: 10.1016/j.margeo.2013.04.018

Ruggiero, P., List, J., Hanes, D., and Eshleman, J. (2007). *PROBABILISTIC SHORELINE CHANGE MODELING*. (Heidelberg, Alemania: Springer Science and Business Media). 3417–3429. doi: 10.1142/9789812709554_0288

SCS. (1956). Hydrology, National Engineering Handbook. Soil Conservation Service. Washington, DC: USDA.

Solari, S., and Losada, M. Á. (2012). Unified distribution models for met-ocean variables: Application to series of significant wave height. *Coast. Eng.* 68, 67–77. doi: 10.1016/j.coastaleng.2012.05.004

Splinter, K. D., and Coco, G. (2021). Challenges and opportunities in coastal shoreline prediction. *Front. Mar. Sci.* 8. doi: 10.3389/fmars.2021.788657

Stockdon, H. F., Holman, R. A., Howd, P. A., and Sallenger, A. H. (2006). Empirical parameterization of setup, swash, and runup. *Coast. Eng.* 53, 573–588. doi: 10.1016/j.coastaleng.2005.12.005

Stripling, S., Panzeri, M., Blanco, B., Rossington, K., Sayers, P., and Borthwick, A. (2017). Regional-scale probabilistic shoreline evolution modelling for flood-risk assessment. *Coast. Eng.* 121, 129–144. doi: 10.1016/j.coastaleng.2016.12.002

Thiéblemont, R., Le Cozannet, G., Rohmer, J., Toimil, A., Álvarez-Cuesta, M., and Losada, I. J. (2021). Deep uncertainties in shoreline change projections: an extraprobabilistic approach applied to sandy beaches. *Natural Hazards. Earth Syst. Sci.* 21, 2257–2276. doi: 10.5194/nhess-21-2257-2021

Toimil, A., Álvarez-Cuesta, M., and Losada, I. J. (2023). Neglecting the effect of longand short-term erosion can lead to spurious coastal flood risk projections and maladaptation. *Coast. Eng.* 179. doi: 10.1016/j.coastaleng.2022.104248

Toimil, A., Camus, P., Losada, I. J., and Álvarez-Cuesta, M. (2021). Visualising the uncertainty cascade in multi-ensemble probabilistic coastal erosion projections. *Front. Mar. Sci.* 8. doi: 10.3389/fmars.2021.683535

Toimil, A., Losada, I. J., Camus, P., and Díaz-Simal, P. (2017). Managing coastal erosion under climate change at the regional scale. *Coast. Eng.* 128, 106–122. doi: 10.1016/j.coastaleng.2017.08.004

Toimil, A., Losada, I. J., Nicholls, R. J., Dalrymple, R. A., and Stive, M. J. F. (2020). Addressing the challenges of climate change risks and adaptation in coastal areas: A review. *Coast. Eng.* 156. doi: 10.1016/j.coastaleng.2019.103611

Torrecillas, C., Payo, A., Cobos, M., Burke, H., Morgan, D., Smith, H., et al. (2024). Sediment thickness model of andalusia's nearshore and coastal inland topography. *J. Mar. Sci. Eng.* 12. doi: 10.3390/jmse12020269

Usoskin, I. G., Mursula, K., Solanki, S., Schüssler, M., and Alanko, K. (2004). Reconstruction of solar activity for the last millennium using 10Be data. *Astronomy. Astrophys.* 413, 745–751. doi: 10.1051/0004-6361:20031533

van Maanen, B., Nicholls, R. J., French, J. R., Barkwith, A., Bonaldo, D., Burningham, H., et al. (2016). Simulating mesoscale coastal evolution for decadal coastal management: A new framework integrating multiple, complementary modelling approaches. *Geomorphology* 256, 68–80. doi: 10.1016/j.geomorph.2015.10.026

Vitousek, S., Barnard, P. L., Limber, P., Erikson, L., and Cole, B. (2017). A model integrating long-shore and cross-shore processes for predicting long-term shoreline response to climate change. *J. Geophys. Res.: Earth Surface.* 122, 782–806. doi: 10.1002/2016JF004065

Vitousek, S., Cagigal, L., Montaño, J., Rueda, A., Mendez, F., Coco, G., et al. (2021). The application of ensemble wave forcing to quantify uncertainty of shoreline change predictions. *J. Geophys. Res.: Earth Surface.* 126. doi: 10.1029/2019JF005506

Vrijling, J. K., and Meijer, G. J. (1992). Probabilistic coastline position computations. Coast. Eng. 17, 1–23. doi: 10.1016/0378-3839(92)90011-I

Wainwright, D. J., Ranasinghe, R., Callaghan, D. P., Woodroffe, C. D., Jongejan, R., Dougherty, A. J., et al. (2015). Moving from deterministic towards probabilistic coastal hazard and risk assessment: Development of a modelling framework and application to Narrabeen Beach, New South Wales, Australia. *Coast. Eng.* 96, 92–99. doi: 10.1016/j.coastaleng.2014.11.009

Wang, B., and Reeve, D. (2010). Probabilistic modelling of long-term beach evolution near segmented shore-parallel breakwaters. Coast. Eng. 57, 732–744. doi: 10.1016/ j.coastaleng.2010.03.004

Wilcock, P., and Crowe, J. (2003). Surface-based transport model for mixed-size sediment. *J. Hydraulic. Eng.* 129 (2), 120–128. doi: 10.1061/ASCE0733-94292003129:2120

Yang, W., Yang, H., Yang, D., and Hou, A. (2020). Causal effects of dams and land cover changes on flood changes in mainland China. *Hydrol. Earth Syst. Sci. Discuss.* 2020, 1–21. doi: 10.5194/hess-2020-609

Zacharioudaki, A., and Reeve, D. E. (2011). Shoreline evolution under climate change wave scenarios. *Clim. Change* 108, 73–105. doi: 10.1007/s10584-010-0011-7